

Solving Structured Hierarchical Games Using Differential Backward Induction

Zun Li, Feiran Jia, Aditya Mate, Shahin Jabbari, Mithun Chakraborty
Milind Tambe, Yevgeniy Vorobeychik

October 12, 2021

Abstract

From large-scale organizations to decentralized political systems, hierarchical strategic decision making is commonplace. We introduce a novel class of *structured hierarchical games (SHGs)* that formally capture such hierarchical strategic interactions. In an SHG, each player is a vertex in a tree, and strategic choices of players are sequenced from root to leaves, with root moving first, followed by its children, then followed by their children, and so on until the leaves. A player’s utility in an SHG depends on its own decision, and on the choices of its parent and *all* the tree leaves. SHGs thus generalize simultaneous-move games, as well as Stackelberg games with many followers. We leverage the structure of both the sequence of player moves as well as payoff dependence to develop a novel gradient-based back propagation-style algorithm, which we call *Differential Backward Induction (DBI)*, for approximating equilibria of SHGs. We then provide a sufficient condition for convergence of DBI. Finally, we demonstrate the efficacy of the proposed algorithmic approach in finding approximate equilibrium solutions to several classes of SHGs.

1 Introduction

The COVID-19 pandemic has revealed considerable strategic tension among the many parties involved in decentralized hierarchical policy-making. For example, recommendations by the World Health Organization are sometimes heeded, and other times discarded by nations, while subnational units, such as provinces and urban areas, may in turn take a policy stance (such as on lockdowns, mask mandates, or vaccination priorities) that is not congruent with national policies. Similarly, in the U.S., policy recommendations at the federal level can be implemented in a variety of ways by the states, while counties and cities, in turn, may comply with state-level policies, or not, potentially triggering litigation [18]. Central to all these cases is that, besides this strategic drama, what ultimately determines infection spread is how policies are implemented *at the lowest level*, such as by cities and towns, or even individuals. Similar strategic encounters routinely play out in large-scale organizations, where actions throughout the management hierarchy are ultimately reflected in the decisions made at the lowest level (e.g., by the employees who are ultimately involved in production), and these lowest-level decisions play a decisive role in the organizational welfare.

We propose a novel model of hierarchical decision making which is a natural stylized representation of strategic interactions of this kind. Our model, which we term *structured hierarchical games (SHGs)*, represents each player by a node in a tree hierarchy. The tree plays two roles in SHGs. First, it captures the sequence of moves by the players: the root (the lone member of level 1 of the hierarchy) makes the first strategic choice, its children (i.e., all nodes in level 2) observe the root’s choice and follow, their children then follow in turn, and so on, until we reach the leaf node players who move upon observing their parents’ choices. Second, the tree partially captures strategic dependence: a player’s utility depends on its own strategy, that of its parent, and the strategies of *all of the leaf nodes*. The sequence of moves in our model naturally captures the typical sequence of decisions in hierarchical policy-making settings, as well as in large organizations, while the utility structure captures the decisive role of leaf nodes (e.g., individual compliance with vaccination policies), as well as hierarchical dependence (e.g., employee dependence on a manager’s approval of their performance, or

state dependence on federal funding). Crucially, the *SHG* model generalizes a number of well-established models of strategic encounters, including (a) simultaneous-move games (captured by a 2-level SHG with the root having a single dummy action), (b) Stackelberg (leader-follower) games (a 2-level game with a single leaf node) [13, 45], and (c) single-leader multi-follower Stackelberg games (e.g., a Stackelberg security game with a single defender and many attackers) [7, 9].

Our second contribution is a novel gradient-based algorithm for approximately computing subgame-perfect equilibria of *SHGs*. Specifically, we propose *Differential Backward Induction (DBI)*, which is a backpropagation-style gradient ascent algorithm that leverages both the sequential structure of the game, as well as the utility structure of the players. As *DBI* involves simultaneous gradient updates of players in the same level (particularly at the leaves), convergence is not guaranteed in general (as is also the case for best-response dynamics [14]). Viewing *DBI* as a dynamical system, we provide a sufficient condition for its convergence to a stable point. Our results also imply that in the special case of two-player zero-sum Stackelberg games, *DBI* converges to a local Stackelberg equilibrium [13, 47]. Finally, we demonstrate the efficacy of *DBI* in finding approximate equilibrium solutions to several classes of *SHGs*.

The rest of this paper is organized as follows. We review the related work in the remainder of this section. In Section 2.1, we formally define the class of *SHGs*. We introduce our algorithm, *DBI*, and analyze its convergence properties in Section 3. Section 4 is dedicated to our experimental results on various *SHG*. We wrap up by a discussion in Section 5.

1.1 Related Work

SHGs generalize Stackelberg games [45] with multiple followers [7, 27], encompass graphical games [23] and contain simultaneous-move games as a special case.

There have been several approaches that use gradient-based methods for solving games with particular structures. One of the most important examples is the learning of generative adversarial networks (GANs) [16], which are modeled as zero-sum games [22]. A common approach for training GANs is via simultaneous gradient-ascent-descent (GDA) [38]. However, to speed up convergence as well as to tackle the potential cyclic behavior of basic GDA, advanced versions of GDA leverage ideas such as optimistic gradient [10] and extragradient [36], and reconstruction of the gradient dynamics through spectrum analysis [37]. These ideas have been adopted in gradient-based approaches to solve multi-player general-sum games [8, 26, 35], where spectrum-based methods [6, 20] are shown to outperform the basic GDA for a class of multi-player games, and specific methods are designed for multi-player games that admit a monotonic gradient structure [30, 36]. However, all of these approaches assume a fully simultaneous game setting.

The closest thread to our work considers gradient-based methods for bi-level optimization [29, 43]. Both Fiez et al. [13] and Wang et al. [47] consider Stackelberg games, and also use the implicit function theorem to derive gradient updates. We generalize these ideas by considering a more general hierarchical game structure. Other applications include learning quantal response equilibrium in Stackelberg games for gradient learners [3], Stackelberg security games [40], combinatorial optimization [49], optimization on graphs [50], mechanism design [28], model-based reinforcement learning [42], and learning game structure from behavior data [31, 32]. However, all of these approaches focus on a two-level hierarchy which is a special case of our model.

Our work bears high-level similarities to the recent trend of *implicit deep learning* [2, 4, 17] — optimization problems pipelined into network structures. This allows learning algorithms to be derived using the optimality conditions. Applications of implicit deep learning include meta-learning [25, 41], deep equilibrium models [5], hyperparameter optimization [34] and auxiliary learning [39].

Very recently, Wang et al. [46] proposed a gradient based approach for Stackelberg games but their main focus is to deal with multiplicity of equilibria. Finally, Jia et al. [21] study a stylized 3-level SHG for pandemic policy making. We compare with their approach in Section 4.

2 Structured Hierarchical Games

We use bold lower-case letters to denote vectors. Let f be a function of the form $f(\mathbf{x}, \mathbf{y}) : \mathbb{R}^d \times \mathbb{R}^{d'} \rightarrow \mathbb{R}^{d''}$. We use $\nabla_{\mathbf{x}} f$ to denote the partial derivative of f with respect to \mathbf{x} . When there is functional dependency between \mathbf{x} and \mathbf{y} , we use $D_{\mathbf{x}} f$ to denote the total derivative of $f(\mathbf{x}, \mathbf{y}(\mathbf{x}))$ with respect to \mathbf{x} . We use $\nabla_{\mathbf{x}, \mathbf{x}}^2 f$ and $\nabla_{\mathbf{x}, \mathbf{y}}^2 f$ to denote the second-order partial derivatives and $D_{\mathbf{x}, \mathbf{x}}^2 f$ to denote the second-order total derivative of f . For a mapping $f : \mathbb{R}^d \rightarrow \mathbb{R}^d$, we use $f^t(\mathbf{x})$ to denote t iterative applications of f on \mathbf{x} . For mappings $f_1 : \mathbb{R}^d \rightarrow \mathbb{R}^d$ and $f_2 : \mathbb{R}^d \rightarrow \mathbb{R}^d$, we define $(f_1 \circ f_2)(\mathbf{x}) \triangleq f_1(f_2(\mathbf{x}))$ and $(f_1 + f_2)(\mathbf{x}) \triangleq f_1(\mathbf{x}) + f_2(\mathbf{x})$. Finally, for a given $\epsilon \in \mathbb{R}^{\geq 0}$ and $\mathbf{x} \in \mathbb{R}^d$, we define the ϵ -ball around \mathbf{x} as $\mathbb{B}_{\epsilon}(\mathbf{x}) = \{\mathbf{x}' \in \mathbb{R}^d \mid \|\mathbf{x} - \mathbf{x}'\|_2 < \epsilon\}$. Finally, \mathbf{I} denotes an identity matrix.

2.1 Formal Model

A structured hierarchical game (SHG) \mathcal{G} of L layers consists of $n_l \geq 1$ players at the l -th layer (see Figure 1). We use (l, i) to denote the index of the i -th player at layer l , with some canonical player order within each layer. Denote the set of players by \mathcal{N} . Players are organized such that each player at layer l has a unique

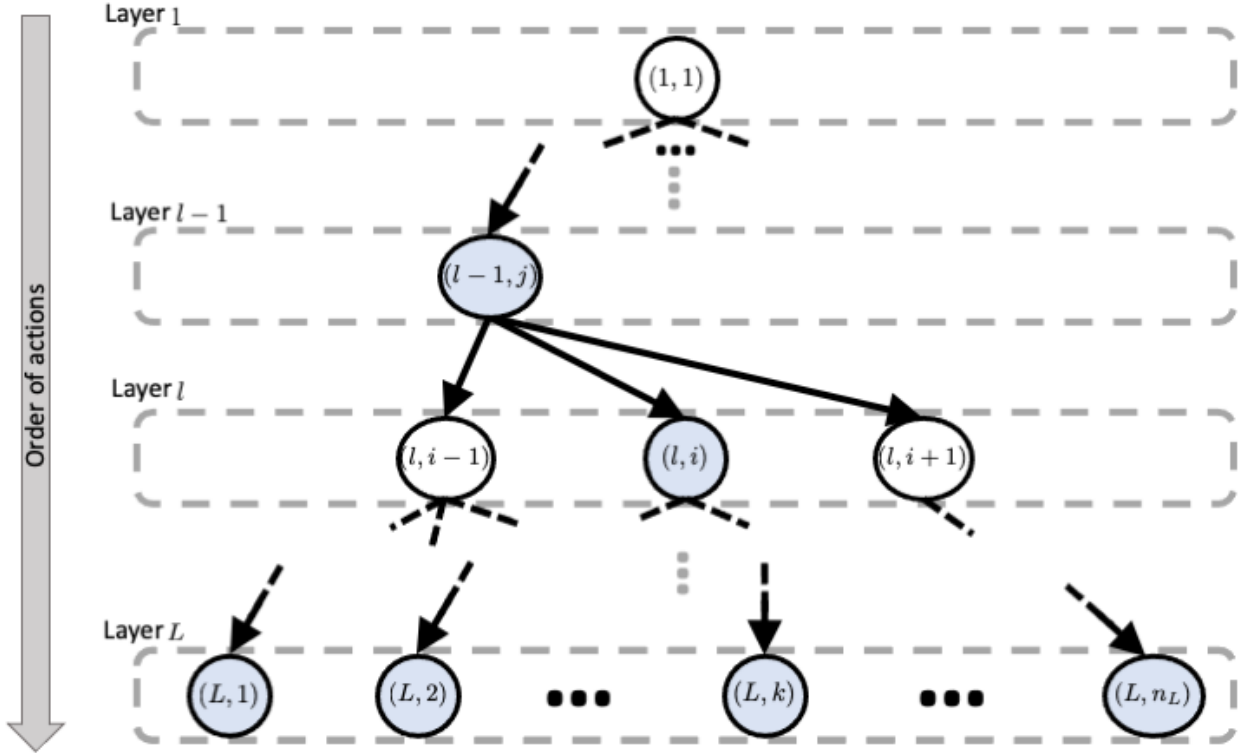


Figure 1: Schematic representation of an SHG. The utility of player (l, i) can have direct functional dependence *only* on the joint action of *all* shaded players.

parent at layer $l - 1$. We use $\text{PA}(l, i)$ to denote the parent of (l, i) and $\text{CHD}(l, i)$ to denote the set of its immediate descendants (or children). Without loss of generality, we assume $n_1 = 1$ so that the game structure can be represented by a rooted tree.¹ We use $\text{DES}(l, i)$ to denote the set of descendants of (l, i) (excluding (l, i)), and $\text{LEAF}(l, i)$ to denote all the layer- L players that are descendants of (l, i) .

We use $\mathcal{X}_{l,i} \subseteq \mathbb{R}^{d_{l,i}}$ to denote the set of actions available to player (l, i) . The game operates in a sequential manner over layers: the layer-1 player $(1, 1)$ selects an action $\mathbf{x}_{1,1} \in \mathcal{X}_{1,1}$. Given this choice of action, all

¹We can add a dummy player with a singleton action set $\mathcal{X}_{1,1}$ as the parent of all original layer-1 players.

players $(2, i)$ in layer 2 simultaneously select their own actions $\mathbf{x}_{2,i} \in \mathcal{X}_{2,i}$ and so on up to the players in the last layer L .

Let \mathbf{x}_l denote the joint action of all players in layer l and $\mathbf{x}_{l,-i}$ the joint action of all players in layer l except player (l, i) i.e. $\mathbf{x}_l := \langle \mathbf{x}_{l,i}, \mathbf{x}_{l,-i} \rangle$ where $\langle \cdot, \cdot \rangle$ represents a concatenation. We assume player (l, i) receives a payoff of the form $u_{l,i}(\mathbf{x}_{l,i}, \mathbf{x}_{\text{PA}(l,i)}, \mathbf{x}_L)$ i.e., the payoff can only depend on player's action, its parent's action, and the actions of the players in the last layer. This assumption is applicable to many SHGs. For example, in our pandemic policy motivating example in the introduction, the assumption implies that the utility of an actor e.g., a state is determined by the state's own policy, the policy of its parent i.e., the federal government which can impose non-compliance penalties to the state and the policies deployed at the lowest level e.g., local businesses and which determine the spread of infection as well as the level of economic recovery. See Section 4 for more details.

Note that the SHG model is quite general. In particular, SHGs generalize simultaneous-move games, as well as Stackelberg games with many followers. For simultaneous-move games, we can construct a 2-level SHG with a root node that has a single dummy action. A general 2-level SHG, on the other hand, is a Stackelberg game with one or many followers. In terms of utility dependencies, SHGs are related to *graphical games* [23] as we can view each player as having a directed edge towards its parents and every last-layer player. However, graphical games are simultaneous-move games, whereas the structure of SHGs captures a sequential nature of moves across layers.

Remark 1. The simultaneous-move assumption for players within the same level is for ease of exposition. Both our solution concept and algorithm are applicable to the setting where the players within the same level select their actions asynchronously as long as each player selects its action after observing its parent's action, knowing that all utilities are realized only after all players have selected their actions.

2.2 Solution Concept

As a sequential game, the natural solution concept for SHGs is the *subgame perfect equilibrium* (SPE). We start by formally defining the subgame.

Definition 1 (Subgames in SHG). *For an SHG \mathcal{G} and a player (l, i) , given a joint action profile \mathbf{x} , the subgame $\mathcal{G}_{l,i}(\mathbf{x})$ is an SHG rooted at (l, i) defined only by player (l, i) and its descendants $\text{DES}(l, i)$, while fixing the actions of other players as in \mathbf{x} that are in \mathcal{G} but not in $\mathcal{G}_{l,i}(\mathbf{x})$.*

Given the definition above, a strategy profile $\mathbf{x}^* = (\mathbf{x}_1^*, \dots, \mathbf{x}_L^*)$ is a *subgame perfect equilibrium* (SPE) for \mathcal{G} if its restriction to every subgame $\mathcal{G}_{l,i}(\mathbf{x}^*)$ of \mathcal{G} is a Nash equilibrium for $\mathcal{G}_{l,i}(\mathbf{x}^*)$. Backward induction is the classic paradigm for solving for an SPE. However, vanilla backward induction in extensive-form games generally requires discrete action spaces. Furthermore, computing equilibria is generally intractable for general-sum multi-player games [11]. These make solving for an SPE in SHGs with continuous action spaces and non-zero sum utilities a hard problem which has no known general solutions. Next, we propose the first general algorithm for solving SHGs with continuous strategy spaces (including mixed strategies in finite-action games) and differentiable utility functions.

3 Differential Backward Induction

In this section, we describe our algorithm, Differential Backward Induction (DBI), for computing an SPE, and then analyze its convergence. Before formally defining DBI, let us introduce some notation. For a player (l, i) , let $\phi_{l,i} : \mathbb{R}^{d_{\text{PA}(l,i)}} \rightarrow \mathbb{R}^{d_{l,i}}$ denote its *local* best response given the action of its parent. For any player (L, i) in the last layer L , this means if $\phi_{L,i}(\mathbf{x}_{\text{PA}(L,i)}) = \mathbf{x}_{L,i}$ then $\nabla_{\mathbf{x}_{L,i}} u_{L,i}(\mathbf{x}_{L,i}, \mathbf{x}_{\text{PA}(L,i)}, \langle \mathbf{x}_{L,i}, \mathbf{x}_{L,-i} \rangle) = 0$ and $\nabla_{\mathbf{x}_{L,i}, \mathbf{x}_{L,i}}^2 u_{L,i}(\mathbf{x}_{L,i}, \mathbf{x}_{\text{PA}(L,i)}, \langle \mathbf{x}_{L,i}, \mathbf{x}_{L,-i} \rangle) < 0$.² Since the utility functions can be nonconvex, ϕ only returns a local best response (local optimal) solution instead of a global one. Moreover, let $\phi_l : \mathbb{R}^{d_{l-1}} \rightarrow \mathbb{R}^{d_l}$ denote the

²For simplicity, we omit degenerate cases where $\nabla_{\mathbf{x}_{L,i}, \mathbf{x}_{L,i}}^2 u_{L,i} = 0$; we assume all local maxima are strict.

local best response for all the players in layer l given the actions of the players in layer $l-1$ where $d_l = \sum_i d_{l,i}$. We can then compose these local best response functions to define the function $\Phi_l := \phi_L \circ \phi_{L-1} \circ \dots \circ \phi_{l+1} : \mathbb{R}^{d_l} \rightarrow \mathbb{R}^{d_l}$ i.e., the local best response of players in the last layer L given the actions of the players in layer l .³ This implies that for any player (l, i) where $l < L$, $D_{\mathbf{x}_{l,i}} u_{l,i}(\mathbf{x}_{l,i}, \mathbf{x}_{\text{PA}(l,i)}, \Phi_l(\langle \mathbf{x}_{l,i}, \mathbf{x}_{l,-i} \rangle)) = 0$ and $D_{\mathbf{x}_{l,i}}^2 u_{l,i}(\mathbf{x}_{l,i}, \mathbf{x}_{\text{PA}(l,i)}, \Phi_l(\langle \mathbf{x}_{l,i}, \mathbf{x}_{l,-i} \rangle)) < 0$, where $D_{\mathbf{x}_{l,i}}$ is the total derivative with respect to $\mathbf{x}_{l,i}$ (as $\Phi_l(\langle \mathbf{x}_{l,i}, \mathbf{x}_{l,-i} \rangle)$ is also a function of $\mathbf{x}_{l,i}$). Similar to ϕ , Φ also returns a local best response instead of a global one. The functions ϕ, Φ are implicit functions capturing the functional dependencies between actions of players in different layers at the local equilibrium.

Throughout, we make the following standard assumption on the utility functions [12, 47].

Assumption 1. *For any $\mathbf{x}_{l,i} \in \mathcal{X}_{l,i}$, the second-order partial derivatives of the form $\nabla_{\mathbf{x}_{l,i}, \mathbf{x}_{l,i}}^2 u_{l,i}$ are non-singular.*

3.1 Algorithm

The algorithm works in a bottom-up manner: For each layer l , we compute the total derivatives (gradients) of the utility functions and local best response maps (ϕ, Φ) based on analytical expressions that we derive below, and propagate this information back to the higher layer $l-1$; we also update each player's action by a step proportional to its utility gradient with respect to its own action. We analyze the properties of differential backward induction in light of the theory of dynamical systems.

Algorithm 1 Differential Backward Induction (DBI)

Input: An SHG instance \mathcal{G}

Parameters: Learning rate α , maximum number of iterations T for gradient update

Output: A strategy profile

```

Randomly initialize  $\mathbf{x}^0 = \langle \mathbf{x}_1^0, \dots, \mathbf{x}_L^0 \rangle$  ▷ Initialization
for  $t = 1, 2, \dots, T$  do ▷ Loop over number of gradient update iterations
  for  $l = L, L-1, \dots, 1$  do ▷ Backward induction loop
    for  $i = 1, 2, \dots, n_l$  do ▷ Loop over players in the layer
      if  $l = L$  then ▷ Check for the last-level players
        Back-propagate  $\mathbf{I}$  as  $D_{\mathbf{x}_{L,i}} \Phi_{L,i}$  to  $\text{PA}(L, i)$  ▷  $\Phi_{L,i} = \phi_{L,i} = \mathbf{x}_{L,i}$ 
        Set  $\mathbf{x}_{L,i}^t \leftarrow \mathbf{x}_{L,i}^{t-1} + \alpha \nabla_{\mathbf{x}_{L,i}} u_{L,i}$  ▷ Gradient update step
      else
        Compute  $\nabla_{\mathbf{x}_{l,i}} u_{l,i}, \nabla_{\mathbf{x}_L} u_{l,i}$  at  $\mathbf{x}^{t-1}$ 
        Compute  $D_{\mathbf{x}_{l,i}} \phi_{l+1,j}, \forall (l+1, j) \in \text{CHD}(l, i)$  from Equation (4)
        Compute  $D_{\mathbf{x}_{l,i}} \Phi_l$  using  $D_{\mathbf{x}_{l+1,j}} \Phi_{l+1,j}$  propagated below ▷ Equation (3)
        Back-propagate  $D_{\mathbf{x}_{l,i}} \Phi_l$  to  $\text{PA}(l, i)$ 
        Compute  $D_{\mathbf{x}_{l,i}} u_{l,i} = \nabla_{\mathbf{x}_{l,i}} u_{l,i} + \nabla_{\mathbf{x}_L} u_{l,i} D_{\mathbf{x}_{l,i}} \Phi_l$ 
        Set  $\mathbf{x}_{l,i}^t \leftarrow \mathbf{x}_{l,i}^{t-1} + \alpha D_{\mathbf{x}_{l,i}} u_{l,i}$  ▷ Gradient update step
    Return  $\mathbf{x}^T$  ▷ Output after  $T$  iterations

```

We now derive analytical expressions for the above total derivatives of players at different levels. We start from the last layer L . Given the actions of players directly above (i.e., \mathbf{x}_{L-1}), for player (L, i) , its total derivative with respect to its own action is simply equal to the partial derivative i.e.,

$$D_{\mathbf{x}_{L,i}} u_{L,i}(\mathbf{x}_{L,i}, \mathbf{x}_{\text{PA}(L,i)}, \langle \mathbf{x}_{L,i}, \mathbf{x}_{L,-i} \rangle) = \nabla_{\mathbf{x}_{L,i}} u_{L,i}. \quad (1)$$

For layer $L-1$, the total derivative for player $(i, L-1)$ at an equilibrium is

$$D_{\mathbf{x}_{L-1,i}} u_{L-1,i}(\mathbf{x}_{L-1,i}, \mathbf{x}_{\text{PA}(L-1,i)}, \phi_L(\langle \mathbf{x}_{L-1,i}, \mathbf{x}_{L-1,-i} \rangle)) = \nabla_{\mathbf{x}_{L-1,i}} u_{L-1,i} + (\nabla_{\mathbf{x}_L} u_{L-1,i})(D_{\mathbf{x}_{L-1,i}} \phi_L),$$

³Note that in particular $\Phi_L = \phi_L$.

where $\nabla_{\mathbf{x}_L} u_{L-1,i}$ is a $1 \times d_L$ vector and $D_{\mathbf{x}_{L-1,i}} \phi_L$ is a $d_L \times d_{L-1,i}$ matrix. The technical challenge here is to derive the term $D_{\mathbf{x}_{L-1,i}} \phi_L$. Recall that ϕ_L is the vectorized concatenation of the $\phi_{L,j}$ functions. And since in our model a player in layer L is only directly affected by its direct parent at layer $L-1$, the only terms in ϕ_L that depend on $\mathbf{x}_{L-1,i}$ are the actions of $\text{CHD}(L-1, i)$. So it only suffices to derive $D_{\mathbf{x}_{L-1,i}} \phi_{L,j}$ for players $(L, j) \in \text{CHD}(L-1, i)$. For these players (L, j) , $\nabla_{\mathbf{x}_{L,j}} u_{L,j} = 0$. Our next goal is to extract the infinitesimal dependencies between $\mathbf{x}_{L-1,i}$ and $\mathbf{x}_{L,j}$ through this first-order condition. A technical tool we use is the implicit function theorem.

Theorem 1 (Implicit Function Theorem [12, Theorem 1B.1]). *Let $f(\mathbf{x}_1, \mathbf{x}_2) : \mathbb{R}^{d_1} \times \mathbb{R}^{d_2} \rightarrow \mathbb{R}^{d_2}$ be a continuously differentiable function in a neighborhood of $(\mathbf{x}_1^*, \mathbf{x}_2^*)$ such that $f(\mathbf{x}_1^*, \mathbf{x}_2^*) = 0$. Also suppose $\nabla_{\mathbf{x}_2} f$, the Jacobian of f with respect to \mathbf{x}_2 , is non-singular at $(\mathbf{x}_1^*, \mathbf{x}_2^*)$. Then around a neighborhood of \mathbf{x}_1^* , we have a local diffeomorphism $\mathbf{x}_2^*(\mathbf{x}_1) : \mathbb{R}^{d_1} \rightarrow \mathbb{R}^{d_2}$ such that $D_{\mathbf{x}_1} \mathbf{x}_2 = -(\nabla_{\mathbf{x}_2} f)^{-1} \nabla_{\mathbf{x}_1} f$.*

To use Theorem 1, we set $f = \nabla_{\mathbf{x}_{L,j}} u_{L,j}$ (which satisfies the conditions of Theorem 1 by Assumption 1), $\mathbf{x}_1 = \mathbf{x}_{L-1,i}$ and $\mathbf{x}_2 = \mathbf{x}_{L,j}$. Then the theorem implies that there is a local diffeomorphism $\phi_{L,j} : \mathcal{X}_{L-1,i} \rightarrow \mathcal{X}_{L,j}$ defined by

$$D_{\mathbf{x}_{L-1,i}} (\nabla_{\mathbf{x}_{L,j}} u_{L,j} (\phi_{L,j}(\mathbf{x}_{L-1,i}), \mathbf{x}_{L-1,i}, \langle \mathbf{x}_{L,j}, \mathbf{x}_{L,-j} \rangle)) = 0.$$

This gives us

$$(\nabla_{\mathbf{x}_{L,j}, \mathbf{x}_{L,j}}^2 u_{L,j}) (D_{\mathbf{x}_{L-1,i}} \phi_{L,j}) + \nabla_{\mathbf{x}_{L,j}, \mathbf{x}_{L-1,i}}^2 u_{L,j} = 0 \implies D_{\mathbf{x}_{L-1,i}} \phi_{L,j} = -(\nabla_{\mathbf{x}_{L,j}, \mathbf{x}_{L,j}}^2 u_{L,j})^{-1} \nabla_{\mathbf{x}_{L,j}, \mathbf{x}_{L-1,i}}^2 u_{L,j}.$$

Define $\nabla_{L,j}^2 := \nabla_{\mathbf{x}_{L,j}, \mathbf{x}_{L-1,i}}^2 u_{L,j}$. Then we can have a complete analytical form for

$$\begin{aligned} & (\nabla_{\mathbf{x}_L} u_{L-1,i}) (D_{\mathbf{x}_{L-1,i}} \phi_L) \\ &= - \sum_{(L,j) \in \text{CHD}(L-1,i)} (\nabla_{\mathbf{x}_{L,j}} u_{L-1,i}) D_{\mathbf{x}_{L-1,i}} \phi_{L,j} = - \sum_{(L,j) \in \text{CHD}(L-1,i)} (\nabla_{\mathbf{x}_{L,j}} u_{L-1,i}) (\nabla_{\mathbf{x}_{L,j}, \mathbf{x}_{L,j}}^2 u_{L,j})^{-1} \nabla_{L,j}^2. \end{aligned}$$

Replacing back to Equation (2), we get that

$$D_{\mathbf{x}_{L-1,i}} u_{L-1,i} (\mathbf{x}_{L-1,i}, \mathbf{x}_{\text{PA}(L-1,i)}, \phi_L(\mathbf{x}_{L-1,i})) = \nabla_{\mathbf{x}_{L-1,i}} u_{L-1,i} - \sum_{(L,j) \in \text{CHD}(L-1,i)} (\nabla_{\mathbf{x}_{L,j}} u_{L-1,i}) (\nabla_{\mathbf{x}_{L,j}, \mathbf{x}_{L,j}}^2 u_{L,j})^{-1} \nabla_{L,j}^2. \quad (2)$$

For layer $l < L-1$, the total derivative of player (l, i) again at an equilibrium is

$$D_{\mathbf{x}_{l,i}} u_{l,i} = \nabla_{\mathbf{x}_{l,i}} u_{l,i} + (\nabla_{\mathbf{x}_L} u_{l,i}) (D_{\mathbf{x}_{l,i}} \Phi_l),$$

where

$$D_{\mathbf{x}_{l,i}} \Phi_l = (D_{\mathbf{x}_{l+1}} \Phi_{l+1}) (D_{\mathbf{x}_{l,i}} \mathbf{x}_{l+1}) = \sum_{(l+1,j) \in \text{CHD}(l,i)} (D_{\mathbf{x}_{l+1,j}} \Phi_{l+1}) (D_{\mathbf{x}_{l,i}} \phi_{l+1,j}). \quad (3)$$

We can again apply Theorem 1 to get

$$D_{\mathbf{x}_{l,i}} \phi_{l+1,j} = -(\nabla_{\mathbf{x}_{l+1,j}, \mathbf{x}_{l+1,j}}^2 u_{l+1,j})^{-1} \nabla_{\mathbf{x}_{l+1,j}, \mathbf{x}_{l,i}}^2 u_{l+1,j}, \quad (4)$$

for $j \in \text{CHD}(l, i)$. So we apply the above procedure recursively for $D_{\mathbf{x}_{l+1}} \Phi_{l+1}$ to derive the total derivative for players (l, i) where $l < L-1$.

$$D_{\mathbf{x}_{l,i}} u_{l,i} = \nabla_{\mathbf{x}_{l,i}} u_{l,i} + \left(\sum_{(L,j) \in \text{LEAF}(l,i)} (-1)^{L-l} \nabla_{\mathbf{x}_{L,j}} u_{L,i} \prod_{(\lambda,\eta) \in \text{PATH}((L,j) \rightarrow (l,i))} (\nabla_{\mathbf{x}_{\lambda,\eta}, \mathbf{x}_{\lambda,\eta}}^2 u_{\lambda,\eta})^{-1} \nabla_{\mathbf{x}_{\lambda,\eta}, \mathbf{x}_{\text{PA}(\lambda,\eta)}}^2 u_{\lambda,\eta} \right), \quad (5)$$

where $\text{PATH}((L, j) \rightarrow (l, i))$ is an ordered list of nodes lying on the unique path from (L, j) to (l, i) , excluding (l, i) . Note that Equation (5) is a generalization of Equation (2) where the PATH only consists of the leaf vertex.

We can thus compute the quantities $D_{\mathbf{x}_{l,i}} u_{l,i}$ that we use in our iterative, bottom-up gradient-based Algorithm 1 by Equation (1) if $l = L$ and otherwise use Equation (5). Note, that Algorithm 1 essentially works in a backward message-passing manner: after each player has computed its total derivative, it back-propagates $D_{\mathbf{x}_{l,i}} \Phi_l$ to its direct parent; this information is, in turn, used by the parent to compute its own total derivative. We emphasize that although the above derivation assumes the ϕ, Φ functions are exact local best responses, in our algorithm in each iteration we evaluate these functional expressions for the total derivatives at the current joint action profile. This largely reduces computational complexity and ensures that Algorithm 1 satisfies the first-order conditions upon convergence.

3.2 Convergence Analysis

In this section, we study the convergence properties of DBI to stable points. We first note that convergence is not guaranteed in general, since SHGs generalize simultaneous-move games, and updates in that special case amount to gradient-based better-response dynamics which may lead to cycles [14].

To study convergence of DBI, we first observe that the gradient updates in Algorithm 1 can be interpreted as a discrete dynamical system, $\mathbf{x}^{t+1} = F(\mathbf{x}^t)$, with $F(\mathbf{x}^t) = (\mathbf{I} + \alpha G)(\mathbf{x}^t)$ where G is an update gradient vector. This system is an approximation of the continuous limit dynamical system $\dot{\mathbf{x}} = G(\mathbf{x})$ when $\alpha \rightarrow 0$. A standard solution concept for such dynamical systems is captured by the following definition.

Definition 2 (LASP [15]). *A continuous (or discrete) dynamical system $\dot{\mathbf{x}} = G(\mathbf{x})$ (or $\mathbf{x}^{t+1} = F(\mathbf{x}^t)$) has a locally asymptotic stable point (LASP) \mathbf{x}^* if $\exists \epsilon > 0, \lim_{t \rightarrow \infty} \mathbf{x}^t = \mathbf{x}^*, \forall \mathbf{x}^0 \in \mathbb{B}_\epsilon(\mathbf{x}^*)$.*

There are well-known sufficient and necessary conditions for the existence of an LASP.

Proposition 1 (Characterization of LASP [48, Theorem 1.2.5, Theorem 3.2.1]). *A point \mathbf{x}^* is an LASP for the continuous dynamical system $\dot{\mathbf{x}} = G(\mathbf{x})$ if $G(\mathbf{x}^*) = 0$ and all eigenvalues of Jacobian matrix $\nabla_{\mathbf{x}} G$ at \mathbf{x}^* have negative real parts. Furthermore, for any \mathbf{x}^* such that $G(\mathbf{x}^*) = 0$, if $\nabla_{\mathbf{x}} G$ has eigenvalues with positive real parts at \mathbf{x}^* , then by the stable manifold theorem [48, Theorem 3.2.1] \mathbf{x}^* cannot be an LASP.*

The existence of an LASP depends on the game structure. Regardless, we show that for an SHG, DBI reaches an LASP in the limit if such a point exists. For all results of this section, we recall that the utility functions of \mathcal{G} satisfy Assumption 1. Furthermore, we use $\dot{\mathbf{x}} = G(\mathbf{x})$ to denote the continuous dynamical system corresponding to \mathcal{G} and assume that this dynamical system has an LASP that satisfies the sufficient conditions of Proposition 1. We defer all the omitted proofs to Appendix B.

Proposition 2. *Let $\lambda_1, \dots, \lambda_d$ denote the eigenvalues of the updating Jacobian $\nabla_{\mathbf{x}} G$ at an LASP \mathbf{x}^* and define $\lambda^* = \arg \max_{i \in [d]} \text{Re}(\lambda_i) / |\lambda_i|^2$, where Re is the real part operator. Then with a learning rate $\alpha < -2\text{Re}(\lambda^*) / |\lambda^*|^2$, and an initial point $\mathbf{x}^0 \in \mathbb{B}_\epsilon(\mathbf{x}^*)$ for some $\epsilon > 0$ around \mathbf{x}^* , DBI converges to an LASP. Specifically, if the choice of learning rate equals α^* and the modulus of matrix $\rho(\mathbf{I} + \alpha^* \nabla_{\mathbf{x}} G) = 1 - \kappa < 1$, then the dynamics converge to \mathbf{x}^* with the rate of $O((1 - \kappa/2)^t)$.*

Proposition 2 states that there exists a region such that, if the initial point is in that region, then DBI will converge to an LASP. We next show that if we assume first-order Lipschitzness for the update rule, then we can also characterize the region of initial points which converge to an LASP.

Proposition 3. *Suppose G is L -Lipschitz.⁴ Then for all $\mathbf{x}^0 \in \mathbb{B}_{\kappa/2L}(\mathbf{x}^*)$, $\epsilon > 0$ and after T rounds of gradient update, DBI will output a point $\mathbf{x}^T \in \mathbb{B}_\epsilon(\mathbf{x}^*)$ as long as $T \geq \lceil \frac{2}{\kappa} \log \|\mathbf{x}^0 - \mathbf{x}^*\| / \epsilon \rceil$ where κ is as defined in Proposition 2.*

We further show that through random initialization, the probability of reaching a *saddle point* is 0.

⁴Formally, this means that $\exists L > 0$ such that $\forall \mathbf{x}, \mathbf{x}' \in \mathcal{X}, \|G(\mathbf{x}) - G(\mathbf{x}')\|_2 \leq L \|\mathbf{x} - \mathbf{x}'\|_2$.

Proposition 4. Suppose G is L -Lipschitz. Let $\alpha < 1/L$ and define the saddle points of the dynamics G as $\mathcal{X}_{sad}^* = \{\mathbf{x}^* \in \mathcal{X} \mid \mathbf{x}^* = (\mathbf{I} + \alpha G)(\mathbf{x}^*), \rho((\mathbf{I} + \alpha \nabla_{\mathbf{x}} G)(\mathbf{x}^*)) > 1\}$. Also let $\mathcal{X}_{sad}^0 = \{\mathbf{x}^0 \in \mathcal{X} \mid \lim_{t \rightarrow \infty} (\mathbf{I} + \alpha G)^t(\mathbf{x}^0) \in \mathcal{X}_{sad}^*\}$ denote the set of initial points that converge to a saddle point. Then $\mu(\mathcal{X}_{sad}^0) = 0$, where μ is Lebesgue measure.

Recall that we designed DBI to compute an (approximate) SPE. In Section 4, we empirically study the relationship between LASP and SPE and also compare DBI with other baselines for several SHGs.

4 Experiments

In this section, we empirically investigate the following questions: (1) the convergence rate of our algorithm (2) the solution quality of our algorithm (3) the behavior of our algorithm in games where we can verify global stability.

4.1 Convergence Analysis

We start by investigating the convergence behaviors of our algorithm as well as some baselines on different instances of SHGs. We compare DBI with simultaneous partial gradient ascent (SIM) [8, 35], symplectic gradient dynamics with or without alignment (SYM_ALN and SYM, respectively) [6], consensus optimization (CO) [37] and Hamilton gradient (HAM) [1, 33]. SIM, SYM_ALN, SYM, CO and HAM are all designed to compute a local Nash equilibrium [6, 8].

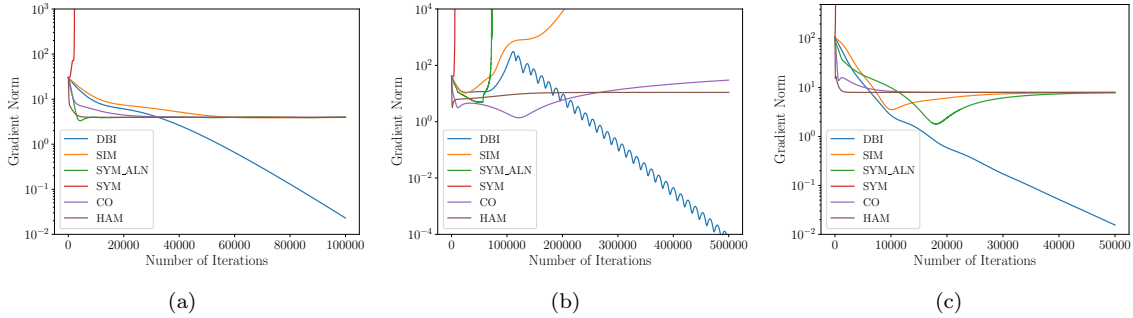


Figure 2: Convergence behaviors on (a) a (1, 1, 1) game with 1-d actions (b) a (1, 1, 2) game with 1-d actions (c) a (1, 1, 1) game with 3-d actions.

We test on three SHG instances with different game properties: (a) a three-layer chain structure (or the (1, 1, 1) game) with 1-d actions (b) a “ λ ” shape tree (or the (1, 1, 2) game) with 1-d action spaces, and (c) and (1, 1, 1) game with 3-d actions. In all the games, the payoffs are polynomial functions of \mathbf{x} with randomly generated coefficients. Details are in Appendix B. We run all algorithm with the same initial point and learning rate. The results are shown in Figure 2 where we plot the L_2 norm of total gradient for each of the algorithms (Y axis) against the number of iterations (X axis).

In all cases DBI converges to a critical point that meets the first-order conditions while baseline algorithms fail to do so. This is not surprising since baseline methods are designed to meet the first-order condition of a local Nash equilibrium and not an LASP. In scenarios (a) and (c), all baselines have converged to a point with finite norm for the total gradients. In (b), however, only CO and HAM converge to a stationary point while SIM, SYM, SYM_ALN all diverge. For scenario (b), DBI appears to be on an inward spiral to a critical point. We further check the second-order condition (details in Appendix B) and verify that DBI has converged to local maxima of individual payoffs in all three games.

4.2 Local Solution Qualities

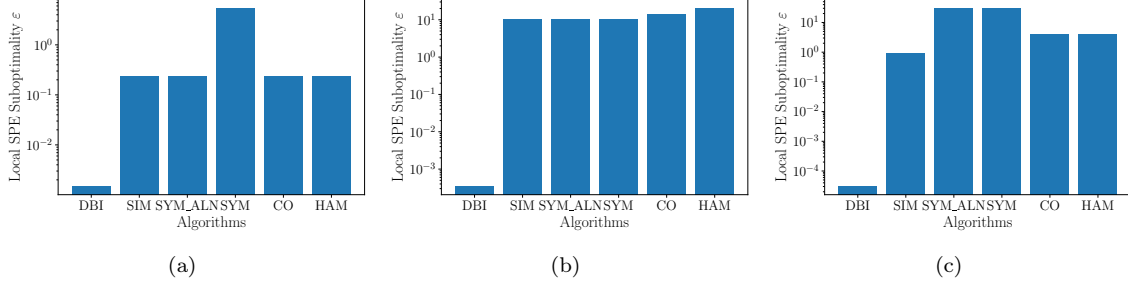


Figure 3: Solution qualities on (a) a $(1, 1, 1)$ game with 1-d actions (b) a $(1, 1, 2)$ game with 1-d actions (c) a $(1, 1, 1)$ game with 3-d actions.

We will now study the solution quality of our algorithm. Normally in games we evaluate the stability of a strategy profile \mathbf{x} by considering the maximum individual deviation in payoffs (called regret of the \mathbf{x} which we denote by $\varepsilon(\mathbf{x})$). However due to the sequentiality and the specific information structure of SHGs, when player (l, i) deviates we should also take account of the strategic effects propagated to the subgame $\mathcal{G}_{l,i}(\mathbf{x})$. i.e., when $\mathbf{x}_{l,i}$ changes we should also re-equilibrate $\mathcal{G}_{l,i}(\mathbf{x})$. However for multidimensional non-compact action spaces and non-convex payoffs, computing for $\varepsilon(\mathbf{x})$ globally is generally intractable. Therefore for this case we approximate ε locally by reusing our DBI algorithm.

To be more specific, when we compute the regret of \mathbf{x} , we first enumerate each individual player (l, i) , and run DBI only on $\mathcal{G}_{l,i}(\mathbf{x})$ from \mathbf{x} until convergence. Then we define the regret of player (l, i) as the deviation in payoffs between (l, i) 's original payoff and its payoff in the new resulting profile. And then we define $\varepsilon(\mathbf{x})$ as the maximum of such ε across all players. We consider this evaluation approach to fully exploit the tractability of the gradient ascent algorithm and approximate the ground-truth regret locally to a fair degree.

As shown in Figure 4, across all three game instances DBI outputs a near-zero regret profile while other algorithm fails. This demonstrates the ability of DBI in terms of reaching equilibria locally.

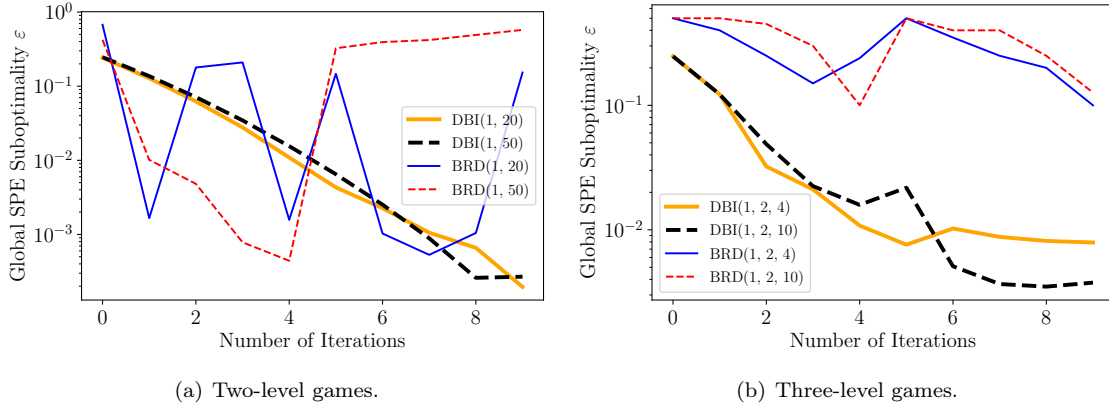


Figure 4: Results on COVID-19 Game Models. Note that the definitions of a single iteration of an algorithm are on different scales for DBI and BRD (see Appendix B for details).

4.3 Global Solution Qualities on A Class of Structured Game Model

We next consider a class of SHGs where we can tractably verify the global stability of a solution, and check whether our algorithm converges to such a global equilibrium. Specifically, we investigate a class of games inspired by COVID-19 policy-making [21]. The hierarchy has layers corresponding to the (single) federal government, multiple state governments, and county administrations under each state. Each player’s action (policy) is to set a social-distancing factor which is a number in $[0, 1]$, and its cost (or negative payoff) is a convex combination (with respect to idiosyncratic weights) of the new fraction of infections after policy intervention, socio-economic cost of the policy implementation, and compliance cost with its parent. See Appendix B for details.

Since the actions are in a one-dimensional compact space and the depth of the hierarchy is at most 3, we use grid search (over the discretized interval $[0, 1]$) along with Algorithm 2 in Appendix B (labeled BRD) to compute an approximate SPE as well as a measure the *global* ε of any given solution. We include the computational details in Appendix B. We compare DBI against a top-down version of BRD, and measure the ε -s of the outputs over iterations, as shown in Figure 4. The curve labeled DBI(1, 20) corresponds to results from running DBI on a (1, 20) structured game; other plot legends are similarly defined.

The plots show that generally DBI converges to a *global* equilibrium for this class of games, whereas BRD is likely to cycle in the action space — this is most prominent from the high volatility of ε -values over iterations for two-level games in Figure 4(a). In other words, although our algorithm is designed for finding equilibria locally, it discovers a global equilibrium in a certain class of games! Figure 4(b) also provides evidence of the scalability of our approach: as we increase the number of players and layers, DBI converges in a smaller amount of time than BRD to a good solution (see Appendix B for details).

5 Discussion

We introduced a novel class of hierarchical games, proposed a new game-theoretic solution concept and designed an algorithm to compute it. We assume a specific form of utility dependency between players and our solution concept only guarantees local stability. Improvement on each of these two fronts is an interesting direction for future work.

Given the generality of our framework, our approach can be used for many applications characterized by a hierarchy of strategic agents e.g., pandemic policy making. However, our modeling requires the full knowledge of the true utility functions of all players and our analysis assumes full rationality for all the players. Although the model we have addressed here is already challenging, these assumptions are unlikely to hold in many real-world applications. Therefore, further analysis is necessary to fully gauge the robustness of our approach before deployment.

References

- [1] Jacob Abernethy, Kevin Lai, and Andre Wibisono. Last-iterate convergence rates for min-max optimization: convergence of Hamiltonian gradient descent and consensus optimization. In *Thirty-Second International Conference on Algorithmic Learning Theory*, pages 3–47, 2021.
- [2] Akshay Agrawal, Brandon Amos, Shane Barratt, Stephen Boyd, Steven Diamond, and Zico Kolter. Differentiable convex optimization layers. In *Thirty-Third Conference on Neural Information Processing Systems*, pages 9558–9570, 2019.
- [3] Kareem Amin, Satinder Singh, and Michael Wellman. Gradient methods for Stackelberg security games. In *Thirty-Second Conference on Uncertainty in Artificial Intelligence*, pages 2–11, 2016.
- [4] Brandon Amos and Zico Kolter. OptNet: Differentiable optimization as a layer in neural networks. In *Thirty-Fourth International Conference on Machine Learning*, pages 136–145, 2017.

- [5] Shaojie Bai, Zico Kolter, and Vladlen Koltun. Deep equilibrium models. In *Thirty-Third International Conference on Neural Information Processing Systems*, pages 690–701, 2019.
- [6] David Balduzzi, Sebastien Racaniere, James Martens, Jakob Foerster, Karl Tuyls, and Thore Graepel. The mechanics of n -player differentiable games. In *Thirty-Fifth International Conference on Machine Learning*, pages 354–363, 2018.
- [7] Nicola Basilico, Stefano Coniglio, and Nicola Gatti. Methods for finding leader-follower equilibria with multiple followers. In *Fifteenth International Conference on Autonomous Agents and Multiagent Systems*, pages 1363–1364, 2016.
- [8] Benjamin Chasnov, Lillian Ratliff, Eric Mazumdar, and Samuel Burden. Convergence analysis of gradient-based learning in continuous games. In *Thirty-Sixth Conference on Uncertainty in Artificial Intelligence*, pages 935–944, 2020.
- [9] Stefano Coniglio, Nicola Gatti, and Alberto Marchesi. Computing a pessimistic stackelberg equilibrium with multiple followers: The mixed-pure case. *Algorithmica*, 82(5):1189–1238, 2020.
- [10] Constantinos Daskalakis and Ioannis Panageas. The limit points of (optimistic) gradient descent in min-max optimization. In *Thirty-Second International Conference on Neural Information Processing Systems*, pages 9256–9266, 2018.
- [11] Constantinos Daskalakis, Paul Goldberg, and Christos Papadimitriou. The complexity of computing a Nash equilibrium. *SIAM Journal on Computing*, 39(1):195–259, 2009.
- [12] Asen Dontchev and Tyrrell Rockafellar. *Implicit functions and solution mappings*. Springer, 2009.
- [13] Tanner Fiez, Benjamin Chasnov, and Lillian Ratliff. Implicit learning dynamics in Stackelberg games: Equilibria characterization, convergence analysis, and empirical study. In *Thirty-Seventh International Conference on Machine Learning*, pages 3133–3144, 2020.
- [14] Drew Fudenberg, Fudenberg Drew, David K Levine, and David K Levine. *The theory of learning in games*, volume 2. MIT press, 1998.
- [15] Oded Galor. *Discrete dynamical systems*. Springer Science & Business Media, 2007.
- [16] Ian Goodfellow, Jean Pouget-Abadie, Mehdi Mirza, Bing Xu, David Warde-Farley, Sherjil Ozair, Aaron Courville, and Yoshua Bengio. Generative adversarial networks. In *Twenty-Seventh Conference on Neural Information Processing Systems*, pages 2672–2680, 2014.
- [17] Stephen Gould, Basura Fernando, Anoop Cherian, Peter Anderson, Rodrigo Santa Cruz, and Edison Guo. On differentiating parameterized argmin and argmax problems with application to bi-level optimization. *CoRR*, abs/1607.05447, 2016.
- [18] Michael Hill and Frederic Varone. *The public policy process*. Routledge, 2021.
- [19] Roger Horn and Charles Johnson. *Matrix analysis*. Cambridge University Press, 2012.
- [20] Adam Ibrahim, Waiss Azizian, Gauthier Gidel, and Ioannis Mitliagkas. Linear lower bounds and conditioning of differentiable games. In *Thirty-Seventh International Conference on Machine Learning*, pages 4583–4593, 2020.
- [21] Feiran Jia, Aditya Mate, Zun Li, Shahin Jabbari, Mithun Chakraborty, Milind Tambe, Michael Wellman, and Yevgeniy Vorobeychik. A game-theoretic approach for hierarchical policy-making. *CoRR*, abs/2102.10646, 2021.

- [22] Chi Jin, Praneeth Netrapalli, and Michael Jordan. What is local optimality in nonconvex-nonconcave minimax optimization? In *Thirty-Seventh International Conference on Machine Learning*, pages 4880–4889, 2020.
- [23] Michael Kearns, Michael Littman, and Satinder Singh. Graphical models for game theory. In *Seventeenth Conference on Uncertainty in Artificial Intelligence*, pages 253–260, 2001.
- [24] John Kelley. *General topology*. Springer, 1955.
- [25] Kwonjoon Lee, Subhansu Maji, Avinash Ravichandran, and Stefano Soatto. Meta-learning with differentiable convex optimization. In *IEEE/CVF Conference on Computer Vision and Pattern Recognition*, pages 10657–10665, 2019.
- [26] Alistair Letcher. On the impossibility of global convergence in multi-loss optimization. In *Ninth International Conference on Learning Representations*, 2021.
- [27] Sven Leyffer and Todd Munson. Solving multi-leader-follower games. *Preprint ANL/MCS-P1243-0405*, 2005.
- [28] Jiayang Li, Jing Yu, Yu Nie, and Zhaoran Wang. End-to-end learning and intervention in games. In *Thirty-Fourth Conference on Neural Information Processing Systems*, 2020.
- [29] Shu Li and Tamer Başar. Distributed algorithms for the computation of noncooperative equilibria. *Automatica*, 23(4):523–533, 1987.
- [30] Tianyi Lin, Zhengyuan Zhou, Panayotis Mertikopoulos, and Michael Jordan. Finite-time last-iterate convergence for multi-agent learning in games. In *Thirty-Seventh International Conference on Machine Learning*, pages 6161–6171, 2020.
- [31] Chun Kai Ling, Fei Fang, and Zico Kolter. What game are we playing? End-to-end learning in normal and extensive form games. In *Twenty-Seventh International Joint Conference on Artificial Intelligence*, pages 396–402, 2018.
- [32] Chun Kai Ling, Fei Fang, and Zico Kolter. Large scale learning of agent rationality in two-player zero-sum games. In *Thirty-Third AAAI Conference on Artificial Intelligence*, pages 6104–6111, 2019.
- [33] Nicolas Loizou, Hugo Berard, Alexia Jolicoeur-Martineau, Pascal Vincent, Simon Lacoste-Julien, and Ioannis Mitliagkas. Stochastic Hamiltonian gradient methods for smooth games. In *Thirty-Seventh International Conference on Machine Learning*, pages 6370–6381, 2020.
- [34] Jonathan Lorraine, Paul Vicol, and David Duvenaud. Optimizing millions of hyperparameters by implicit differentiation. In *Twenty-Third International Conference on Artificial Intelligence and Statistics*, pages 1540–1552, 2020.
- [35] Eric Mazumdar, Lillian Ratliff, and Shankar Sastry. On gradient-based learning in continuous games. *SIAM Journal on Mathematics of Data Science*, 2(1):103–131, 2020.
- [36] Panayotis Mertikopoulos and Zhengyuan Zhou. Learning in games with continuous action sets and unknown payoff functions. *Mathematical Programming*, 173(1):465–507, 2019.
- [37] Lars Mescheder, Sebastian Nowozin, and Andreas Geiger. The numerics of GANs. In *Thirty-First International Conference on Neural Information Processing Systems*, pages 1823–1833, 2017.
- [38] Vaishnavh Nagarajan and Zico Kolter. Gradient descent GAN optimization is locally stable. In *Thirty-First International Conference on Neural Information Processing Systems*, pages 5591–5600, 2017.
- [39] Aviv Navon, Idan Achituve, Haggai Maron, Gal Chechik, and Ethan Fetaya. Auxiliary learning by implicit differentiation. In *Ninth International Conference on Learning Representations*, 2021.

- [40] Thanh Nguyen, Arunesh Sinha, and He He. Partial adversarial behavior deception in security games. In *Twenty-Ninth International Joint Conference on Artificial Intelligence*, pages 283–289, 2020.
- [41] Aravind Rajeswaran, Chelsea Finn, Sham Kakade, and Sergey Levine. Meta-learning with implicit gradients. In *Thirty-Third Conference on Neural Information Processing Systems*, pages 113–124, 2019.
- [42] Aravind Rajeswaran, Igor Mordatch, and Vikash Kumar. A game theoretic framework for model based reinforcement learning. In *Thirty-Seventh International Conference on Machine Learning*, pages 7953–7963, 2020.
- [43] Amirreza Shaban, Ching-An Cheng, Nathan Hatch, and Byron Boots. Truncated back-propagation for bilevel optimization. In *Twenty-Second International Conference on Artificial Intelligence and Statistics*, pages 1723–1732, 2019.
- [44] Michael Shub. *Global stability of dynamical systems*. Springer, 1987.
- [45] Heinrich Von Stackelberg. *The theory of the market economy*. Oxford University Press, 1952.
- [46] Kai Wang, Lily Xu, Andrew Perrault, Michael Reiter, and Milind Tambe. Coordinating followers to reach better equilibria: End-to-end gradient descent for stackelberg games. *CoRR*, abs/2106.03278, 2021.
- [47] Yuanhao Wang, Guodong Zhang, and Jimmy Ba. On solving minimax optimization locally: A follow-the-ridge approach. In *Eighth International Conference on Learning Representations*, 2020.
- [48] Stephen Wiggins. *Introduction to applied nonlinear dynamical systems and chaos*. Springer Science & Business Media, 2003.
- [49] Bryan Wilder, Bistra Dilkina, and Milind Tambe. Melding the data-decisions pipeline: Decision-focused learning for combinatorial optimization. In *Thirty-Third AAAI Conference on Artificial Intelligence*, pages 1658–1665, 2019.
- [50] Bryan Wilder, Eric Ewing, Bistra Dilkina, and Milind Tambe. End to end learning and optimization on graphs. In *Thirty-Third Conference on Neural Information Processing Systems*, pages 15750–15761, 2019.
- [51] Bryan Wilder, Marie Charpignon, Jackson Killian, Han-Ching Ou, Aditya Mate, Shahin Jabbari, Andrew Perrault, Angel Desai, Milind Tambe, and Maimuna Majumder. Modeling between-population variation in COVID-19 dynamics in Hubei, Lombardy, and New York City. *Proceedings of the National Academy of Sciences*, 117(41):25904–25910, 2020.
- [52] Stephen Wolfram. *The Mathematica*. Cambridge University Press, 1999.

A Omitted Details from Section 3.2

Proof of Proposition 2. The learning dynamics of DBI can be written as $\mathbf{x}^t = (\mathbf{I} + \alpha G)(\mathbf{x}^{t-1})$. Since G has eigenvalues $\lambda_1, \dots, \lambda_d$ at \mathbf{x}^* , the matrix $\mathbf{I} + \alpha \nabla_{\mathbf{x}} G$ at a stationary point \mathbf{x}^* has eigenvalues $1 + \alpha \lambda_1, \dots, 1 + \alpha \lambda_d$. Since the set of LASPs is non-empty, $\text{Re}(\lambda_i) < 0$ for all λ_i . Then for the choice of α^* in the Proposition, the modulus of the Jacobian

$$\rho(\mathbf{I} + \alpha^* \nabla_{\mathbf{x}} G) = \max_{i \in [d]} |1 + \alpha^* \lambda_i| = \max_{i \in [d]} \sqrt{1 + 2\alpha^* \text{Re}(\lambda_i) + (\alpha^*)^2 |\lambda_i|^2} < 1.$$

Proofs for the convergence rate of $O((1 - \kappa/2)^t)$ can be found in previous work (e.g., Fiez et al. [13, Proposition F.1] or Wang et al. [47, Proposition 4])). For completeness, we provide a proof. Since $\rho(\mathbf{I} +$

$\alpha \nabla_{\mathbf{x}} G(\mathbf{x}^*) = 1 - \kappa$, according to Horn and Johnson [19, Lemma 5.6.10], there exists a matrix norm $\|\cdot\|$ such that $\|\mathbf{I} + \alpha \nabla_{\mathbf{x}} G\| < 1 - \kappa + \epsilon$, for $\forall \epsilon > 0$. We choose $\epsilon = \frac{\kappa}{4}$. The Taylor expansion of $(\mathbf{I} + \alpha G)$ at \mathbf{x}^* is

$$(\mathbf{I} + \alpha G)(\mathbf{x}) = (\mathbf{I} + \alpha G)(\mathbf{x}^*) + (\mathbf{I} + \alpha \nabla_{\mathbf{x}} G)(\mathbf{x}^*)(\mathbf{x} - \mathbf{x}^*) + R(\mathbf{x} - \mathbf{x}^*),$$

where $R(\mathbf{x} - \mathbf{x}^*) = o(\|\mathbf{x} - \mathbf{x}^*\|)$. Let $R_1(\mathbf{x} - \mathbf{x}^*) = \frac{1}{\alpha} R(\mathbf{x} - \mathbf{x}^*)$, Then we have $\lim_{\mathbf{x} \rightarrow \mathbf{x}^*} \frac{R_1(\mathbf{x} - \mathbf{x}^*)}{\|\mathbf{x} - \mathbf{x}^*\|} = 0$. Then we can choose $\delta > 0$ such that $\|R_1(\mathbf{x} - \mathbf{x}^*)\| \leq \frac{\kappa}{4} \|\mathbf{x} - \mathbf{x}^*\|$ when $\|\mathbf{x} - \mathbf{x}^*\| < \delta$.

$$\begin{aligned} \|G(\mathbf{x}) - G(\mathbf{x}^*)\| &\leq \|\nabla_{\mathbf{x}} G(\mathbf{x}^*)(\mathbf{x} - \mathbf{x}^*)\| + \|R_1(\mathbf{x} - \mathbf{x}^*)\| \\ &\leq \|\nabla_{\mathbf{x}} G(\mathbf{x}^*)\| \|\mathbf{x} - \mathbf{x}^*\| + \frac{\kappa}{4} \|\mathbf{x} - \mathbf{x}^*\| \\ &\leq (1 - \frac{\kappa}{2}) \|\mathbf{x} - \mathbf{x}^*\|. \end{aligned}$$

This shows the operator $(\mathbf{I} + \alpha G)$ is a contract mapping with contraction constant $(1 - \frac{\kappa}{2})$. Therefore the convergence rate is $O((1 - \kappa/2)^t)$ \square

Before we present the proof of Proposition 3, we state the following lemma.

Lemma 1. *The update gradient vector G is L -Lipchitz if and only if $\|\nabla_{\mathbf{x}} G\| \leq L$ at all $\mathbf{x} \in \mathcal{X}$.*

Proof. First we prove for "if" direction. Consider $\mathbf{x}_1, \mathbf{x}_2 \in \mathcal{X}$,

$$\begin{aligned} G(\mathbf{x}_2) - G(\mathbf{x}_1) &= \int_0^1 \nabla_{\mathbf{x}} G(\mathbf{x}_1 + \tau(\mathbf{x}_2 - \mathbf{x}_1))(\mathbf{x}_2 - \mathbf{x}_1) d\tau \\ \Rightarrow \|G(\mathbf{x}_2) - G(\mathbf{x}_1)\| &= \left\| \int_0^1 \nabla_{\mathbf{x}} G(\mathbf{x}_1 + \tau(\mathbf{x}_2 - \mathbf{x}_1))(\mathbf{x}_2 - \mathbf{x}_1) d\tau \right\| \\ &\leq \left\| \int_0^1 \nabla_{\mathbf{x}} G(\mathbf{x}_1 + \tau(\mathbf{x}_2 - \mathbf{x}_1)) d\tau \right\| \|\mathbf{x}_2 - \mathbf{x}_1\| \\ &\leq \int_0^1 \|\nabla_{\mathbf{x}} G(\mathbf{x}_1 + \tau(\mathbf{x}_2 - \mathbf{x}_1))\| d\tau \|\mathbf{x}_2 - \mathbf{x}_1\| \\ &\leq L \|\mathbf{x}_2 - \mathbf{x}_1\|. \end{aligned}$$

Then we prove for the "only if" direction. Take $\epsilon > 0$, then for $\forall \mathbf{x}_1, \mathbf{x}_2 \in \mathcal{X}$,

$$\begin{aligned} \left\| \int_0^\epsilon (\nabla_{\mathbf{x}} G(\mathbf{x}_1 + \tau \mathbf{x}_2)) \cdot \mathbf{x}_2 d\tau \right\| &= \|G(\mathbf{x}_1 + \epsilon \mathbf{x}_2) - G(\mathbf{x}_1)\| \leq \epsilon L \|\mathbf{x}_2\| \\ \Rightarrow \lim_{\epsilon \rightarrow 0} \frac{\left\| \int_0^\epsilon (\nabla_{\mathbf{x}} G(\mathbf{x}_1 + \tau \mathbf{x}_2)) \cdot \mathbf{x}_2 d\tau \right\|}{\epsilon \|\mathbf{x}_2\|} &= \frac{\|\nabla_{\mathbf{x}} G(\mathbf{x}_1) \cdot \mathbf{x}_2\|}{\|\mathbf{x}_2\|} \leq L. \end{aligned}$$

Since it holds for any \mathbf{x}_2 , it must be $\|\nabla_{\mathbf{x}} G(\mathbf{x}_1)\| \leq L$. And since it applies for any $\mathbf{x}_1 \in \mathcal{X}$, this completes the proof. \square

Proof of Proposition 3. From the proof from Proposition 2 notice that in order to make $\|\mathbf{x}^t - \mathbf{x}^*\| \leq \epsilon$ we only have to let $t \geq \lceil \frac{2}{\kappa} \log \|\mathbf{x}^0 - \mathbf{x}^*\| / \epsilon \rceil$ since now $\|\mathbf{x}^t - \mathbf{x}^*\| \leq (1 - \frac{\kappa}{2})^t \|\mathbf{x}^0 - \mathbf{x}^*\| \leq \exp(-\kappa/2t) \leq \epsilon$. Now we need to characterize the region of initial points that can converge to \mathbf{x}^* by characterizing the maximum possible radius of such initial point to \mathbf{x}^* . Recall in the proof of Proposition 2, this is captured by the parameter δ . On one hand by using the Lipschitzness, we can bound the residual function by

$$\|R_1(\mathbf{x} - \mathbf{x}^*)\| \leq \int_0^1 \|\mathbf{I} + \alpha \nabla_{\mathbf{x}} G(\mathbf{x}^* + \tau(\mathbf{x} - \mathbf{x}^*)) - (\mathbf{I} + \alpha \nabla_{\mathbf{x}} G(\mathbf{x}^*))\| \|\mathbf{x} - \mathbf{x}^*\| d\tau \leq \frac{L}{2} \|\mathbf{x} - \mathbf{x}^*\|^2.$$

On the other hand to maintain this convergence rate we should let $\|R_1(\mathbf{x} - \mathbf{x}^*)\| \leq \frac{\kappa}{4} \|\mathbf{x} - \mathbf{x}^*\|$. Then we simply let $\leq \frac{L}{2} \|\mathbf{x} - \mathbf{x}^*\|^2 \leq \frac{\kappa}{4} \|\mathbf{x} - \mathbf{x}^*\|$ we get an initial point should satisfy $\|\mathbf{x} - \mathbf{x}^*\| \leq \frac{\kappa}{2L}$. \square

To prove Proposition 4, we need a few more machinery.

Proposition 5. *With $\alpha < 1/L$, $\mathbf{I} + \alpha G$ is a diffeomorphism.*

Proof. First we show $(\mathbf{I} + \alpha G)$ is invertible. Suppose $\mathbf{x}_1, \mathbf{x}_2 \in \mathcal{X}$ such that $\mathbf{x}_1 \neq \mathbf{x}_2$ and $(\mathbf{I} + \alpha G)(\mathbf{x}_1) = (\mathbf{I} + \alpha G)(\mathbf{x}_2)$. Then $\mathbf{x}_1 - \mathbf{x}_2 = \alpha(G(\mathbf{x}_2) - G(\mathbf{x}_1))$. And by $\alpha < 1/L$ we have $\|\mathbf{x}_1 - \mathbf{x}_2\| \leq \alpha L \|\mathbf{x}_1 - \mathbf{x}_2\| < \|\mathbf{x}_1 - \mathbf{x}_2\|$, which is a contraction.

Next we show we show its invert function is well-defined on any point of \mathcal{X} . Notice that $\rho(\alpha \nabla_{\mathbf{x}} G) \leq \|\alpha \nabla_{\mathbf{x}} G\| \leq \alpha L < 1$. And notice that since the eigenvalues of $\mathbf{I} + \alpha \nabla_{\mathbf{x}} G$ is the eigenvalues of $\alpha \nabla_{\mathbf{x}} G$ plus 1, the only way that makes $\det(\mathbf{I} + \alpha \nabla_{\mathbf{x}} G) = 0$ is to have one of the eigenvalues of $\alpha \nabla_{\mathbf{x}} G$ to be -1 . This contradicts to $\rho(\alpha \nabla_{\mathbf{x}} G) < 1$. Therefore by the implicit function theorem, $(\mathbf{I} + \alpha G)$ is a local diffeomorphism on any point of \mathcal{X} , and therefore $(\mathbf{I} + \alpha G)^{-1}$ is well defined on \mathcal{X} . \square

Theorem 2 (Center and Stable Manifold [44, Theorem III.7, Chapter 5]). *Suppose $\mathbf{x}^* = h(\mathbf{x}^*)$ is a critical point for the C^r local diffeomorphism $h : \mathcal{X} \rightarrow \mathcal{X}$. Let $\mathcal{X} = \mathcal{X}_s \oplus \mathcal{X}_u$, where \mathcal{X}_s is the stable center eigenspace belonging to those eigenvalues of $\nabla_{\mathbf{x}} h(\mathbf{x}^*)$ whose modulus is no greater than 1, and \mathcal{X}_u is the unstable eigenspace belonging to those whose modulus is greater than 1. Then there exists a C^r embedded disk $W_{loc}^{cs}(\mathbf{x}^*)$ that is tangent to \mathcal{X}_s at \mathbf{x}^* called the local stable center manifold. Moreover there $\exists \epsilon > 0$, $h(W_{loc}^{cs}(\mathbf{x}^*)) \cap \mathbb{B}_{\epsilon}(\mathbf{x}^*) \subset W_{loc}^{cs}$ and $\bigcap_{t=0}^{\infty} h^{-t}(\mathbb{B}_{\epsilon}(\mathbf{x}^*)) \subset W_{loc}^{cs}(\mathbf{x}^*)$.*

Proof of Proposition 4. For $\forall \mathbf{x}^* \in \mathcal{X}_{sad}^*$, let $\epsilon(\mathbf{x}^*) > 0$ be the radius of neighborhood provided by Theorem 2 for diffeomorphism $h = \mathbf{I} + \alpha G$ and point \mathbf{x}^* . Then define $\mathcal{B} = \bigcup_{\mathbf{x}^* \in \mathcal{X}_{sad}^*} \mathbb{B}_{\epsilon(\mathbf{x}^*)}(\mathbf{x}^*)$. And since \mathcal{X} is a subset of Euclidean space so it is second-countable. By Lindelöf's Lemma [24], which stated that every open cover there is a countable subcover, we can actually write $\mathcal{B} = \bigcup_{i=1}^{\infty} \mathbb{B}_{\epsilon(\mathbf{x}_i^*)}(\mathbf{x}_i^*)$ for a countable family of saddle points $\{\mathbf{x}_i^*\}_{i=1}^{\infty} \subseteq \mathcal{X}_{sad}^*$. Therefore for $\forall \mathbf{x}^0 \in \mathcal{X}_{sad}^0$ that converges to a saddle point, it must converge to \mathbf{x}_i^* for some i . And $\exists T(\mathbf{x}^0) > 0$, such that $\forall t > T(\mathbf{x}^0), h^t(\mathbf{x}^0) \in \mathbb{B}_{\epsilon(\mathbf{x}_i^*)}(\mathbf{x}_i^*)$. From Theorem 2 we have $h^t(\mathbf{x}^0) \in W_{loc}^{sc}(\mathbf{x}_i^*)$. Since h is a diffeomorphism on \mathcal{X} we have $\mathbf{x}^0 \in h^{-t}(W_{loc}^{sc}(\mathbf{x}_i^*))$. We furthermore union over all finite time step $\mathbf{x}^0 \in \bigcup_{t=0}^{\infty} h^{-t}(W_{loc}^{sc}(\mathbf{x}_i^*))$. Then we have $\mathcal{X}_{sad}^0 \subseteq \bigcup_{i=1}^{\infty} \bigcup_{t=0}^{\infty} h^{-t}(W_{loc}^{sc}(\mathbf{x}_i^*))$. For each i since \mathbf{x}_i^* is a saddle point, it has an eigenvalue greater than 1, so the dimension of unstable eigenspace $\dim(\mathcal{X}_u(\mathbf{x}_i^*)) \geq 1$. Therefore the dimension of $W_{loc}^{sc}(\mathbf{x}_i^*)$ is less than full dimension. This leads to $\mu(W_{loc}^{sc}(\mathbf{x}_i^*)) = 0$ for any i . Again since h is a diffeomorphism, h^{-1} is locally Lipschitz which are null set preserving. Then $\mu(h^{-t}(W_{loc}^{sc}(\mathbf{x}_i^*))) = 0$ for $\forall i, t$. And since the countable union of measure zero sets is measure zero, $\mu(\bigcup_{i=1}^{\infty} \bigcup_{t=0}^{\infty} h^{-t}(W_{loc}^{sc}(\mathbf{x}_i^*))) = 0$. So $\mu(\mathcal{X}_{sad}^0) = 0$. \square

A.1 Local Subgame Perfect Equilibrium

Our DBI algorithm essentially is designed to satisfy a first order condition $\forall(l, i), D_{\mathbf{x}_{l,i}} u_{l,i} = 0$. If we furthermore impose a second-order condition $\forall(l, i), D_{\mathbf{x}_{l,i}, \mathbf{x}_{l,i}}^2 u_{l,i} < 0$, then at such point every player reaches their local maxima in payoff, which is effectively corresponding to an local equilibrium notion. In fact, in two-level, one-agent each level case this is consistent with the local Stackelberg equilibrium notion in previous literature [13, 47]. We next formally define the notion of local subgame perfect equilibrium (LSPE).

Definition 3 (LSPE). $\mathbf{x}^* = (\mathbf{x}_1^*, \dots, \mathbf{x}_L^*)$ is a local subgame perfect equilibrium (LSPE) if

1. For all players (L, i) at $\mathbf{x}_{L,i}^*$, $\nabla_{\mathbf{x}_{L,i}} u_{L,i}(\mathbf{x}_{L,i}, \mathbf{x}_{PA(L,i)}^*, \mathbf{x}_L^*) = 0$ and $\nabla_{\mathbf{x}_{L,i}, \mathbf{x}_{L,i}}^2 u_{L,i}(\mathbf{x}_{L,i}, \mathbf{x}_{PA(L,i)}^*, \mathbf{x}_L^*) < 0$.
2. For all players (l, i) where $l < L$ at $\mathbf{x}_{l,i}^*$, $D_{\mathbf{x}_{l,i}} u_{l,i}(\mathbf{x}_{l,i}, \mathbf{x}_{PA(l,i)}^*, \Phi_l(< \mathbf{x}_{l,i}, \mathbf{x}_{l,-i}^* >)) = 0$ and $D_{\mathbf{x}_{l,i}, \mathbf{x}_{l,i}}^2 u_{l,i}(\mathbf{x}_{l,i}, \mathbf{x}_{PA(l,i)}^*, \Phi_l(< \mathbf{x}_{l,i}, \mathbf{x}_{l,-i}^* >)) < 0$.

Proposition 2 only guarantees that DBI will find an LASP when there exists one. So a natural question is to characterize the relationship between LSPEs and LASPs. Fiez et al. [13] shows that for two-player zero-sum Stackelberg games, the set of LASPs and the set of LSPEs coincide. Unfortunately, we next show that this is not the case for general SHGs.

Proposition 6. *There exists a SHG \mathcal{G} such that $LSPE(\mathcal{G}) \not\subset LASP(\mathcal{G})$ and $LASP(\mathcal{G}) \not\subset LSPE(\mathcal{G})$.*

Proof of Proposition 6. Consider a two layer game with one player each layer (also the Stackelberg game [13, 47]). Suppose the action for player 1 is x and for 2 is y , where $x, y \in \mathbb{R}$. The analytical form for first-order gradient is

$$D_x y = -\frac{\frac{\partial^2}{\partial y \partial x} u_2}{\frac{\partial^2}{\partial y^2} u_2}, D_x u_1 = \frac{\partial u_1}{\partial x} - \frac{\partial u_1}{\partial y} \frac{\frac{\partial^2}{\partial y \partial x} u_2}{\frac{\partial^2}{\partial y^2} u_2}, \text{ and, } D_y u_2 = \frac{\partial u_2}{\partial y}.$$

The total second-order closed-form is

$$\begin{aligned} D_{x,x}^2 u_1 &= D_x(D_x u_1) = \frac{\partial}{\partial x} D_x u_1 + \left(\frac{\partial}{\partial y} D_x u_1 \right) \cdot D_x y \\ &= \frac{-\frac{\partial}{\partial y} u_1 \frac{\partial^3}{\partial y^3} u_2 (\frac{\partial^2}{\partial x \partial y} u_2)^2}{(\frac{\partial^2}{\partial y^2} u_2)^3} + \frac{\frac{\partial^2}{\partial x \partial y} u_2 (\frac{\partial^2}{\partial y^2} u_1 \frac{\partial^2}{\partial x \partial y} u_2 + 2 \frac{\partial}{\partial y} u_1 \frac{\partial^3}{\partial x \partial y^2} u_2)}{(\frac{\partial^2}{\partial y^2} u_2)^2} \\ &\quad + \frac{-2 \frac{\partial^2}{\partial x \partial y} u_1 \frac{\partial^2}{\partial x \partial y} u_2 + \frac{\partial}{\partial y} u_1 \frac{\partial^3}{\partial x^2 \partial y} u_2}{\frac{\partial^2}{\partial y^2} u_2} + \frac{\partial^2}{\partial x^2} u_1, \text{ and,} \\ D_{y,y}^2 u_2 &= \frac{\partial^2}{\partial y^2} u_2. \end{aligned}$$

The Jacobian matrix of the dynamics of Algorithm 1 is

$$\begin{pmatrix} \nabla_x(D_x u_1) & \nabla_y(D_x u_1) \\ \nabla_x(D_y u_2) & \nabla_y(D_y u_2) \end{pmatrix},$$

Where

$$\begin{aligned} \nabla_x(D_x u_1) &= \frac{\frac{\partial}{\partial y} u_1 \frac{\partial^2}{\partial x \partial y} u_2 \frac{\partial^3}{\partial x \partial y^2} u_2}{(\frac{\partial^2}{\partial y^2} u_2)^2} - \frac{\frac{\partial^2}{\partial x \partial y} u_1 \frac{\partial^2}{\partial x \partial y} u_2 + \frac{\partial}{\partial y} u_1 \frac{\partial^3}{\partial x^2 \partial y} u_2}{\frac{\partial^2}{\partial y^2} u_2} + \frac{\partial^2}{\partial x^2} u_1, \\ \nabla_y(D_x u_1) &= \frac{\frac{\partial}{\partial y} u_1 \frac{\partial^2}{\partial x \partial y} u_2 \frac{\partial^3}{\partial y^3} u_2}{(\frac{\partial^2}{\partial y^2} u_2)^2} - \frac{\frac{\partial^2}{\partial y^2} u_1 \frac{\partial^2}{\partial x \partial y} u_2 + \frac{\partial}{\partial y} u_1 \frac{\partial^3}{\partial x \partial y^2} u_2}{\frac{\partial^2}{\partial y^2} u_2} + \frac{\partial^2}{\partial x \partial y} u_1, \\ \nabla_x(D_y u_2) &= \frac{\partial^2}{\partial x \partial y} u_2, \text{ and,} \\ \nabla_y(D_y u_2) &= \frac{\partial^2}{\partial y^2} u_2. \end{aligned}$$

Then consider payoff function $u_1(x, y) = -8x^4 + 8x^3y - 5x^2y^2 + 5xy^3 + 6y^4 + 3x^3 + 3x^2y + 6xy^2 + 3y^3 - 8x^2 - xy - 3y^2 + 6x$ and $u_2(x, y) = 4x^4 - x^3y + 5x^2y^2 - 10xy^3 + 10y^4 + 7x^3 - 9x^2y - 7xy^2 - 2y^3 - 3x^2 - 9xy - 4y^2 - 7x - 2y$.

We can derive that $D_x u_1 = 6 - 16x + 9x^2 - 32x^3 - y + 6xy + 24x^2y + 6y^2 - 10xy^2 + 5y^3 - ((-9 - 18x - 3x^2 - 14y + 20xy - 30y^2)(-x + 3x^2 + 8x^3 - 6y + 12xy - 10x^2y + 9y^2 + 15xy^2 + 24y^3)) / (-8 - 14x + 10x^2 - 12y - 60xy + 120y^2)$ and $D_y u_2 = -2 - 9x - 9x^2 - x^3 - 8y - 14xy + 10x^2y - 6y^2 - 30xy^2 + 40y^3$. Then there are two critical points $(x_1^*, y_1^*) \approx (-0.35225, 0.09948)$ and $(x_2^*, y_2^*) \approx (-0.175443, -0.188133)$.

At point (x_1^*, y_1^*) , $D_{x,x}^2 u_1 = 28350.9, D_{y,y}^2 u_2 = 0.268741$ the Jacobian $\begin{pmatrix} \nabla_x(D_x u_1) & \nabla_y(D_x u_1) \\ \nabla_x(D_y u_2) & \nabla_y(D_y u_2) \end{pmatrix} \approx \begin{pmatrix} -1464.55 & 1477.72 \\ -5.42229 & 0.268741 \end{pmatrix}$. And it can be verified that it is an LASP but not an LSPE.

At point (x_2^*, y_2^*) , $D_{x,x}^2 u_1 = -3413.93, D_{y,y}^2 u_2 = -0.711531$ the Jacobian $\begin{pmatrix} \nabla_x(D_x u_1) & \nabla_y(D_x u_1) \\ \nabla_x(D_y u_2) & \nabla_y(D_y u_2) \end{pmatrix} \approx \begin{pmatrix} 27.9321 & 661.496 \\ -3.70221 & -0.711531 \end{pmatrix}$. And it can be verified that it is an LSPE but not an LASP. \square

B Omitted Details from Section 4

B.1 Computational Resources

All our code is written in python. We ran our experiments on an Intel(R) Core(TM) i7-7700HQ CPU @ 2.80GHz for Sections 4.1 and B.5, and on an Intel(R) Core(TM) i9-9820X CPU @ 3.30GHz for Section 4.3.

B.2 Derivation of Total Second-Order Derivatives

In our experiments we may need to check the second-order total derivative at a point. This section provides our approach to calculate such quantity.

For player of level L , $D_{\mathbf{x}_{l,i}, \mathbf{x}_{l,i}}^2 u_{l,i} = \nabla_{\mathbf{x}_{l,i}, \mathbf{x}_{l,i}}^2 u_{l,i}$.

For level $l < L$, notice that $D_{\mathbf{x}_{l,i}} u_{l,i}$ is an explicit function of the action variables of players that are descendants of (l, i) . Denote this set of players as $DES(l, i)$ (excluding (l, i)), then we have $D_{\mathbf{x}_{l,i}, \mathbf{x}_{l,i}}^2 u_{l,i} = \nabla_{\mathbf{x}_{l,i}} (D_{\mathbf{x}_{l,i}} u_{l,i}) + \sum_{(\lambda, \eta) \in DES(l, i)} \nabla_{\mathbf{x}_{\lambda, \eta}} (D_{\mathbf{x}_{l,i}} u_{l,i}) D_{\mathbf{x}_{l,i}} \mathbf{x}_{\lambda, \eta}$.

Here $D_{\mathbf{x}_{l,i}} \mathbf{x}_{\lambda, \eta} = (-1)^{\lambda-l} \prod_{\substack{(\lambda', \eta') \in \\ PATH((\lambda, \eta) \\ \rightarrow (l, i))}} \left(\nabla_{\mathbf{x}_{\lambda', \eta'}, \mathbf{x}_{\lambda', \eta'}}^2 u_{\lambda', \eta'} \right)^{-1} \nabla_{\mathbf{x}_{\lambda', \eta'}, \mathbf{x}_{PA(\lambda', \eta')}}^2 u_{\lambda', \eta'}.$

The terms $\nabla_{\mathbf{x}_{l,i}} (D_{\mathbf{x}_{l,i}} u_{l,i})$ and $\nabla_{\mathbf{x}_{\lambda, \eta}} (D_{\mathbf{x}_{l,i}} u_{l,i})$ involve thrice derivatives. In practice we use either numerical finite-difference methods to approximate this value or use symbolic algebra feature in software tools such as Mathematica [52] to calculate the analytical form of this derivative.

B.3 Details of Convergence Analysis Experiments

Setup We compare the following algorithms, such that the gradient update vectors are as follows

DBI: $G^{DBI} = (D_{\mathbf{x}_1} u_1, \dots, D_{\mathbf{x}_n} u_n)$. SIM: $G^{SIM} = (\nabla_{\mathbf{x}_1} u_1, \dots, \nabla_{\mathbf{x}_n} u_n)$. SYM: $G^{SYM} = G^{SIM} + G^{SIM} A^{SIM}$, where $A^{SIM} = (J^{SIM} - (J^{SIM})^T)/2$, and J^{SIM} is the Jacobian matrix of G^{SIM} . HAM: $G^{HAM} = -\nabla_{\mathbf{x}} \|G^{SIM}\|^2$. CO: $G^{CO} = G^{SIM} + \gamma G^{HAM}$, where we let $\gamma = 0.1$ for all experiments. SYM-ALN: $G^{SYM} = G^{SIM} + \zeta G^{SIM} A^{SIM}$, where ζ is the sign of $\frac{1}{2d} (G^{HAM} (G^{SIM})^T) (G^{HAM} (G^{SIM} A^{SIM})^T) + 0.1$.

Experimental Details for (1, 1, 1), 1-d Action Games We use $u_1(x, z) = -7x^2 + 9xz + x - z$, $u_2(x, y, z) = -2y^2 - 4yz - 10x^2 + 2xz - 3z^2 + 4y + 7x - 8z - 8xyz$, and, $u_3(y, z) = -10z^2 - 9yz + 9y^2 - 5z - 2y$. Here (x, y, z) are action variables for players 1, 2, 3. We use the learning rate of $\alpha = 1e - 5$ for all algorithms. We verify that DBI converges to an LSPE $(x, y, z) = (-0.34, 1.85, -1.08)$.

Experimental Details for (1, 1, 2), 1-d Action Games We use $u_1(x, y, z) = -2x^2 - 3xy + y^2 + 5x + 7y + 3xz - 10yz + 5xyz - 6z$, $u_2(w, x, y, z) = 2w^2 - wx - 3wy - 5x^2 + 9xy + 2y^2 + 3w + 5x - 4y + 5z^2 + 8wz + 7xz - 9yz - 10z$, $u_3(w, y, z) = -5y^2 - 8yz + z^2 + 8y - 9z - 2wy - 4wz - w^2 - 8wyz - 2w$, and, $u_4(w, y, z) = -10z^2 - 2yz + 5y^2 - 7z - 6y - 3wz - 8wy - 10wyz + 5w$. Here (x, w, y, z) are action variables for players 1, 2, 3, 4. We use $\alpha = 4e - 6$ for all algorithms. We verify that DBI converges to an LSPE $(x, w, y, z) = (4.70, -2.13, 10.27, 9.93)$.

Experimental Details for (1, 1, 1), 3-d Action Games We use $u_1(\mathbf{x}, \mathbf{z}) = -7 \sum_{i=1}^3 x_i^2 + 9(\sum_{i=1}^3 x_i)(\sum_{i=1}^3 z_i) + \sum_{i=1}^3 x_i - \sum_{i=1}^3 z_i$, $u_2(\mathbf{x}, \mathbf{y}, \mathbf{z}) = -2 \sum_{i=1}^3 y_i^2 - 4(\sum_{i=1}^3 y_i)(\sum_{i=1}^3 z_i) - 10(\sum_{i=1}^3 x_i)(\sum_{i=1}^3 z_i) + 2 \sum_{i=1}^3 x_i^2 - 3 \sum_{i=1}^3 z_i^2 + 4(\sum_{i=1}^3 x_i)(\sum_{i=1}^3 y_i)(\sum_{i=1}^3 z_i) + 7(\sum_{i=1}^3 x_i) - 8(\sum_{i=1}^3 y_i) - 8(\sum_{i=1}^3 z_i)$, and, $u_3(\mathbf{y}, \mathbf{z}) = -10 \sum_{i=1}^3 z_i^2 - 9(\sum_{i=1}^3 y_i)(\sum_{i=1}^3 z_i) + 9 \sum_{i=1}^3 y_i^2 - 5 \sum_{i=1}^3 y_i - 2 \sum_{i=1}^3 z_i$, where $\mathbf{x}, \mathbf{y}, \mathbf{z}$ are action variables of players 1, 2, 3. We use the learning rate $\alpha = 1e - 5$ for all algorithms. We verify that DBI converges to an LSPE $(\mathbf{x}, \mathbf{y}, \mathbf{z}) = ((-0.39, -0.39, -0.39), (0.29, 0.29, 0.29), (-0.58, -0.58, -0.58))$.

The time cost of each algorithm is measured in Table (1)

| | DBI | SIM | SIM_ALN | SYM | CO | HAM |
|------------|------|------|---------|------|------|------|
| (1,1,1)-1d | 1.65 | 1.26 | 5.92 | 1.61 | 4.91 | 4.58 |
| (1,1,2)-1d | 2.93 | 2.07 | 11.9 | 3.57 | 14.9 | 13.3 |
| (1,1,1)-3d | 12.4 | 10.9 | 60.1 | 9.63 | 49.4 | 53.9 |

Table 1: Comparison of the running times of DBI and baselines from experiment 1.

A note on the physical significance of the above utility functions Although our methodology is applicable in principle to any set of agents’ utility function satisfying the definition of SHGs, it is reasonable to ask whether there exists a game model, grounded in some real-world domain, that exhibits the SHG hierarchy as well as the polynomial multi-variable utility structure above. To that end, consider the **COVID-19 Game** delineated below. In the experiments described below, each agent (a policy-maker in a hierarchy such as the federal government, state governments, and county governments) has a non-dimensional action restricted to closed interval $[0, 1]$, interpreted as a social distancing factor due to policy intervention (either recommended or implemented). However, in general, a policy intervention (hence, and agent’s action) may take the form of a multi-dimensional real vector, e.g. factor for social distancing, factor for vaccination roll-out, etc.; hence, in general, the overall cost (negative payoff) of each agent is a function of $2 + n_L$ vectors rather than $2 + n_L$ scalars (corresponding to the agent, its parent, and all leaves) as in Equation (6). Although the actual functional form is not necessarily polynomial, we can always take a polynomial approximation in our model via curve-fitting or a Taylor series expansion. The above polynomial functions would then belong to the resulting class of functions; in our experiments for Convergence Analysis experiments are randomly chosen since the focus of this paper is not on modeling any real-world multi-agent interaction scenario to a high degree of accuracy but on assessing the performance of our algorithm on reasonable models consistent with the SHG structure. This line of thinking can be also applied to the utility functions used in the experiments on the relationship between LASP and LSPE described at the end of the appendix.

B.4 Details of COVID-19 Game Experiments

Global Subgame Perfect Equilibrium in an SHG Before we analyze the COVID-model, we should formally define the notion of global subgame perfect equilibrium in an SHG. Denote the set of players as \mathcal{N} . Roughly speaking, a profile \mathbf{x}^* is an SPE, if for every (l, i) , given actions of players belonging to $\mathcal{N} \setminus (\{(l, i)\} \cup \text{DES}(l, i))$, player (l, i) reaches its maximum payoff by choosing $\mathbf{x}_{l,i}^*$, while assuming $\text{DES}(l, i)$ also had reached an SPE. We only consider pure SPE here so we assume $\mathbf{x}^* \in \mathcal{X}$.

However, there are a couple of issues here. First let’s imagine when solving a two-level games with n_2 players at the second-layer. Given $(1, 1)$ ’s action choice, the problem of computing SPE in the second-layer is equivalent to computing a Nash equilibrium in the second-layer. However, an exact pure Nash equilibrium may not exist. So which profile should we choose to propagate back to $(1, 1)$? To resolve this issue, we define ε -Nash equilibrium.

Definition 4. For a simultaneous-move game, a profile \mathbf{x}^* is an ε -Nash if for any player n , $\forall \mathbf{x}'_n \in \mathcal{X}_n$, $u_n(\mathbf{x}'_n, \mathbf{x}_{-n}^*) \leq u_n(\mathbf{x}^*) + \varepsilon$.

In another word, an ε -Nash is a profile where for every player a unilateral deviation cannot offer benefit more than ε while fixing other’s profile. In the context of our example for the two level game, given $(1, 1)$ ’s action, we select the profile with the minimum ε of the simultaneous-move game defined on layer 2 as an SPE back to $(1, 1)$.

We now generalize this example to formally define the notion of ε -SPE in an SHG. First let us define $\Phi_{l,i}(\mathbf{x}) \in \mathbb{R}^{d_L}$ that returns the equilibrated profile at layer L . In this profile, leaves that are not descendants of (l, i) are fixed in \mathbf{x} , while $\text{LEAF}(l, i)$ moved to a profile that corresponding to an SPE of $\mathcal{G}_{l,i}(\mathbf{x})$ with an minimum ε . Then we define the $\varepsilon_{l,i}(\mathbf{x})$ as $\max_{\mathbf{x}'_{l,i} \in \mathcal{X}_{l,i}} u_{l,i}(\mathbf{x}'_{l,i}, \mathbf{x}_{\text{PA}(l,i)}, \Phi(\mathbf{x}'_{l,i})) - u_{l,i}(\mathbf{x}_{l,i}, \mathbf{x}_{\text{PA}(l,i)}, \Phi(\mathbf{x}_{l,i}))$ and define $\varepsilon(\mathbf{x}) = \max_{l,i} \varepsilon_{l,i}(\mathbf{x})$ as the ε of profile \mathbf{x} in an SHG \mathcal{G} .

Algorithm 2 Procedures for computing ε of profile \mathbf{x} and an algorithm for computing an approximate SPE

Input: An SHG instance \mathcal{G}

Parameters: Best response iterations T

```

procedure SEARCH( $\mathbf{x}, (l, i)$ )
  for  $\mathbf{x}'_{l,i} \in \mathcal{X}_{l,i}$  do
     $u_{l,i}^{re-eq}(\mathbf{x}'_{l,i}), \varepsilon_{DES(l,i)}(\mathbf{x}'_{l,i}), \mathbf{x}^{re-eq(l,i)}(\mathbf{x}'_{l,i}) \leftarrow \text{RE-EQ}((l, i), \mathbf{x} : \mathbf{x}_{l,i} \rightarrow \mathbf{x}'_{l,i})$ 
  Find  $\mathbf{x}^*_{l,i} \leftarrow \arg \max_{\mathbf{x}'_{l,i}} u_{l,i}^{re-eq}(\mathbf{x}'_{l,i})$ 
  return  $\mathbf{x}^*_{l,i}, u_{l,i}^{re-eq}(\mathbf{x}^*_{l,i}), \mathbf{x}^{re-eq(l,i)}(\mathbf{x}^*_{l,i})$ 
end procedure

procedure RE-EQ( $\mathcal{G}, \mathbf{x}, (l, i)$ )
   $\varepsilon \leftarrow 0$ 
  if  $l < L$  then
     $\mathbf{x}, \varepsilon \leftarrow \text{SHG\_SOLVE}((l, i), \mathbf{x})$ 
  return  $u_{l,i}(\mathbf{x}), \varepsilon, \mathbf{x}$ 
end procedure

procedure SHG_SOLVE( $(l, i), \mathbf{x}$ )
   $\mathbf{x}^0 \leftarrow \mathbf{x}$ 
   $\forall (l+1, j) \in \text{CHD}(l, i)$ , replace its action in  $\mathbf{x}^0$  with other random initialization
  for  $t = 1, 2, \dots, T$  do ▷ layer-wise best response
    for  $(l+1, j) \in \text{CHD}(l, i)$  do
       $u_{l+1,j}^{re-eq}, \varepsilon_{DES(l+1,j)}, \mathbf{x}^{re-eq(l+1,j)} \leftarrow \text{RE-EQ}(\mathcal{G}, \mathbf{x}^{t-1}, (l+1, j))$ 
       $\mathbf{x}'_{l+1,j}, u_{l+1,j}^{re-eq-max}, \mathbf{x}^{re-eq-max(l+1,j)} \leftarrow \text{SEARCH}(\mathbf{x}^{t-1}, (l+1, j))$ 
       $\varepsilon_{l+1,j}^{t-1} = \max\{\varepsilon_{DES(l+1,j)}, u_{l+1,j}^{re-eq-max} - u_{l+1,j}^{re-eq}\}$ 
     $\mathbf{x}^t \leftarrow \mathbf{x}^{t-1}$ 
    for  $\forall (l+1, j) \in \text{CHD}(l, i)$  do
      Replace dimensions of  $\mathbf{x}^t$  belonging to  $\text{DES}(l+1, j)$  with the ones in  $\mathbf{x}^{re-eq-max(l+1,j)}$ 
     $\varepsilon_{l+1}^{t-1} \leftarrow \max_i \varepsilon_{l+1,j}^{t-1}$ 
   $t^* \leftarrow \arg \min_t \varepsilon_{l+1}^t$ 
  return  $\mathbf{x}^{t^*}, \varepsilon_{l+1}^{t^*}$ 
end procedure

procedure COMPUTE_ε( $\mathbf{x}$ )
  for  $(l, i)$  do
     $\mathbf{x}^*_{l,i}, u_{l,i}^*, \mathbf{x}^{re-eq(l,i)} \leftarrow \text{SEARCH}(\mathbf{x}, (l, i))$ 
     $\varepsilon_{l,i} \leftarrow u_{l,i}^* - u_{l,i}(\mathbf{x})$ 
  return  $\max_{l,i} \varepsilon_{l,i}$ 
end procedure

```

We next provide an approximate algorithm (see Algorithm 2) to compute ε in an SHG. Pay attention here that $\mathbf{x} : \mathbf{x}_i \rightarrow \mathbf{x}'_i$ means replacing \mathbf{x}_i of \mathbf{x} with \mathbf{x}'_i . The functions in Algorithm 2 operate as follows. The procedure SEARCH takes a given joint profile \mathbf{x} , player index (l, i) and returns a best response profile for a given player (l, i) . Our approach is that for each action in $\mathbf{x}'_{l,i} \in \mathcal{X}_{l,i}$, we re-equilibrate subgames $\mathcal{G}_{l,i}(\mathbf{x} : \mathbf{x}_{l,i} \rightarrow \mathbf{x}'_{l,i})$, and then compute the corresponding payoff. In our actual implementation, we discretize $\mathcal{X}_{l,i}$ in a bucket of grid points, and search within such bucket. The procedure RE-EQ returns the re-equilibrated profile of $\mathcal{G}_{l,i}(\mathbf{x})$ given (l, i) and \mathbf{x} . The procedure SHG_SOLVE solve a simultaneous-move game at layer $l+1$. It applies an iterative best response approach for $\text{CHD}(l, i)$ to generate diverse profiles, and select the one with minimum possible ε . In each iteration, for each $(l+1, j) \in \text{CHD}(l, i)$, it computes its best response action against the previous joint profile \mathbf{x}^{t-1} . And then in the next iteration it replace those descendant-profiles of $(l+1, j)$ in \mathbf{x}^{t-1} by computed re-equilibrated profiles when $(l+1, j)$ selected its best response. Then it will

return the joint profile with the minimum ε found so-far.

To solve the whole game, we just call $\text{SHG_SOLVE}((0, 0), \mathbf{x})$, where \mathbf{x} is some other action profile. To compute the ε of a given profile, we just call $\text{COMPUTE_}\varepsilon$, where it just compute the maximum unilateral deviation for every player using SEARCH to compute the best response action and payoff.

Structured Game Model Inspired by COVID-19 Policy-Making We will now describe in detail the particular subclass of SHGs that we studied in our experiments reported in Section 4.3. This class is based on the SHG proposed in Jia et al. [21] which we describe in detail here. The exposition is in terms of a *cost function* $\mathcal{C}_{l,i}(\mathbf{x}_{l,i}, \mathbf{x}_{\text{PA}(l,i)}, \mathbf{x}_L)$ for each player, which is more natural in this context, rather than the payoff function $u_{l,i}$ introduced in Section 2.1, with the understanding that $u_{l,i} \equiv -\mathcal{C}_{l,i}$.

There are $L = 3$ layers in the hierarchy such that player $(1, 1)$ represents the federal government (or, simply, government), the players $(2, i)$, $i \in \{1, 2, \dots, n_2\}$ are state governments (or, simply, states), and the players $(3, i)$, $i \in \{1, 2, \dots, n_3\}$ are county governments (or, simply, counties) partitioned into groups such that each group shares a single state as a parent.

Each player (l, i) takes a bounded, scalar action $x_{l,i} \in [0, 1]$ which is a *social-distancing factor* that (multiplicatively) reduces the proportion of post-intervention contacts among individuals — a lower number implies a stronger policy intervention, hence a lower number of infections but a higher cost of implementation (see below). The actions taken by counties represent policies that get *actually implemented* (hence directly impact the realized cost of every player — one of the defining attributes of SHGs) while those taken by the government and states are *recommendations*. Similar to Jia et al. [21], we also study a restricted variant where each county is non-strategic and constrained to comply with the action (recommendation) of its parent-state, effectively reducing the model to a 2-layer hierarchy. We call this special case a *two-level game* (Figure 4(a)) and the more general model a *three-level game* (Figure 4(b)).

The cost function of each player (l, i) has, in general, three components: a *policy impact cost* $\mathcal{C}_{l,i}^{\text{inc}}(\mathbf{x}_L)$ which we will elaborate on below; a *policy implementation cost* $\mathcal{C}_{l,i}^{\text{dec}}(\mathbf{x}_L)$, e.g. economic and psychological costs of a lockdown; and, for each player in layers $l > 1$, a *non-compliance cost* $\mathcal{C}_{l,i}^{\text{NC}}(\mathbf{x}_{l,i}, \mathbf{x}_{\text{PA}(l,i)})$, a penalty incurred by a policy-maker for deviating from the recommendation of its parent in the hierarchy (e.g., a fine, litigation costs, or reputation harm).

Let $N_{(3,i)} > 0$ denote the fixed population under the jurisdiction of county $(3, i)$ for every $i \in \{1, 2, \dots, n_3\}$. By construction, the population under each state is given $N_{(2,i)} = \sum_{(3,j) \in \text{CHD}(2,i)} N_{(3,j)}$ and the population under the government is $N_{(1,1)} = \sum_{i=1}^{n_2} N_{(2,i)}$. We next define the expressions for each component of the cost function.

Policy Impact Cost: This cost component is a quadratic closed-form approximation to the agent-based model introduced by Wilder et al. [51]. This is inspired by the infection cost computation approach in Jia et al. [21] but they used a different closed-form approximation. For each each county $(3, i)$, let $N_{(3,i)}^{\text{init}}$ denote the number of infected individuals within the population of the county prior to policy intervention; thus, the number of *post-intervention susceptible* individuals is $(N_{(3,i)} - N_{(3,i)}^{\text{init}})x_{3,i}$. Another parameter in the game is the *transport matrix* $R = \{r_{aa'}\}_{a,a' \in (3,1),(3,2),\dots,(3,n_3)}$, where $r_{aa'} \geq 0$ is the proportion of the population of county a' that is active in county a in the absence of an intervention. Thus, in the number of post-intervention infected individuals of county a' that is active in county a is $r_{aa'} N_{a'}^{\text{init}} x_{a'}$. The last parameter in the model is M , the average number of contacts with active individuals that a susceptible individual makes, and finally μ is the probability that a susceptible individual gets infected upon contact with an active infected individual is $\mu \in (0, 1)$.

Putting these together, the policy impact cost is defined by the fraction of post-intervention infected individuals in county $a = (3, i)$, $i \in \{1, 2, \dots, n_3\}$:

$$\mathcal{C}_a^{\text{inc}}(\mathbf{x}_L) = \mu M x_a \frac{N_a - N_a^{\text{init}}}{N_a^2} \left(\sum_{a'} r_{aa'} N_{a'}^{\text{init}} x_{a'} \right).$$

For a higher-layer player (l, i) ,

$$\mathbf{C}_{l,i}^{\text{inc}}(\mathbf{x}_L) = \frac{1}{N_{(l,i)}} \sum_{a \in \text{CHD}(l,i)} N_a \mathbf{C}_a^{\text{inc}}(\mathbf{x}_L).$$

Policy Implementation Cost: For each county $(3, i)$, the policy implementation cost is given by

$$\mathbf{C}_{3,i}^{\text{dec}}(\mathbf{x}_L) = 1 - x_{3,i}.$$

For a higher-layer player (l, i) ,

$$\mathbf{C}_{l,i}^{\text{dec}}(\mathbf{x}_L) = \frac{1}{N_{(l,i)}} \sum_{a \in \text{CHD}(l,i)} N_a \mathbf{C}_a^{\text{dec}}(\mathbf{x}_L).$$

Non-Compliance Cost: The non-compliance cost of player (l, i) for $l \in \{2, 3\}$ is given by Euclidean distance between its action and that of its parent:

$$\mathbf{C}_{l,i}^{\text{NC}}(x_{l,i}, x_{\text{PA}(l,i)}) = (x_{l,i} - x_{\text{PA}(l,i)})^2.$$

Finally, each player (l, i) for $l > 1$ has an idiosyncratic set of *weights* $\kappa_{l,i} \geq 0$ and $\eta_{l,i} \geq 0$ that trade its three cost components off against each other via a convex combination, and account for differences in ideology; the overall cost of such a player is given by

$$\mathbf{C}_{l,i}(x_{l,i}, x_{\text{PA}(l,i)}, \mathbf{x}_L) = \kappa_{l,i} \mathbf{C}_{l,i}^{\text{inc}}(\mathbf{x}_L) + \eta_{l,i} \mathbf{C}_{l,i}^{\text{dec}}(\mathbf{x}_L) + (1 - \kappa_{l,i} - \eta_{l,i}) \mathbf{C}_{l,i}^{\text{NC}}(x_{l,i}, x_{\text{PA}(l,i)}). \quad (6)$$

The player $(1, 1)$ obviously has no non-compliance issues, hence it has only one weight $\kappa_{1,1} > 0$, its overall cost being

$$\mathbf{C}_{1,1}(x_{1,1}, \mathbf{x}_L) = \kappa_{1,1} \mathbf{C}_{1,1}^{\text{inc}}(\mathbf{x}_L) + (1 - \kappa_{1,1}) \mathbf{C}_{1,1}^{\text{dec}}(\mathbf{x}_L).$$

In our experiments, we set $r_{aa'} = 1/n_3$ for every pair of counties (a, a') , $M = 20$ and $\mu = 0.3$.

Experimental Setup and Further Results We formally define the algorithm BRD as the procedure $\text{SHG_SOLVE}((0, 0), \mathbf{x})$ for some randomly initialized \mathbf{x} . We start by defining the concept of one full *algorithm iteration* for each of DBI and BRD. For DBI(1, 20), DBI(1, 50), DBI(1, 2, 4), DBI(1, 2, 10), one algorithm iteration consists of 50 steps of gradient ascent, with a learning rate of 0.01. For BRD(1, 20) and BRD(1, 50), one algorithm iteration consists of 20 iterations of layer-wise best response during the recursive procedure in SHG_SOLVE ; for BRD(1, 2, 4) and BRD(1, 2, 10), it corresponds to 500 and 200 iterations of layer-wise best response, respectively. For DBI we adopt a projector operator that project the resulted action into the nearest point in $[0, 1]$.

We discretize each action space uniformly into 101 grid points for two-level games, and 11 grid points for three-level games. We let $T = 100$ for BRD(1, 20) and BRD(1, 50) and $T = 20$ for BRD(1, 2, 4) and BRD(1, 2, 10). In the three-level experiments, the κ is set to be 0.5 for counties and the states and 0.8 for the government. The η is set to be 0.2 for the states, 0.3 for the counties in (1,2,4) setting, and 0.2 for (1,2,10) experiment. In the two-level experiments, the κ is set to be 0.2 for the government, 0.5 for counties and the states. The η is set to be 0.2 for counties and states.

Figure 5 shows the running times for the experiments that corresponding to Figure 4. It should be noted that the number of players has more effects on the run-time of BRD compared to DBI.

To further study the scalability of the BRD and DBI algorithms, we compare the run-time that (1) the DBI algorithm converges and (2) the BRD algorithm terminates. The convergence of DBI is defined as the convergence of the action profile. When DBI converges, the action profile remains unchanged. In the

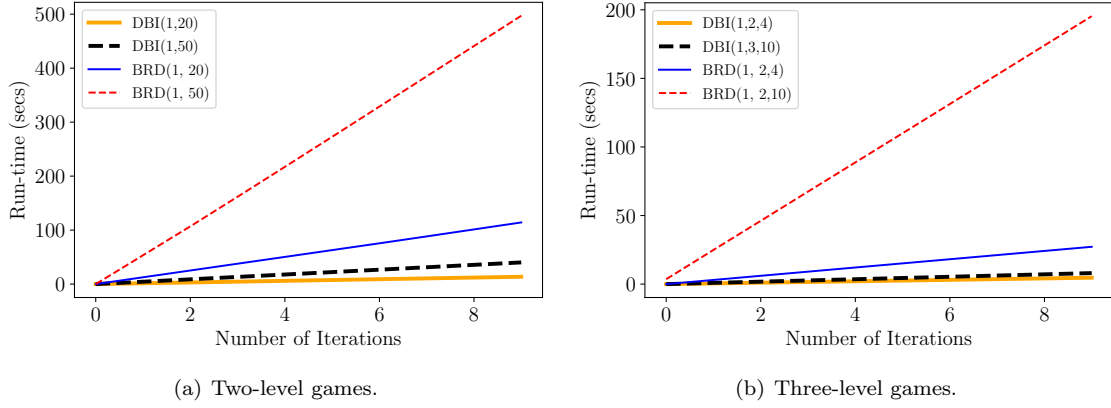


Figure 5: Run-time (in secs) results on COVID-19 Game Models.

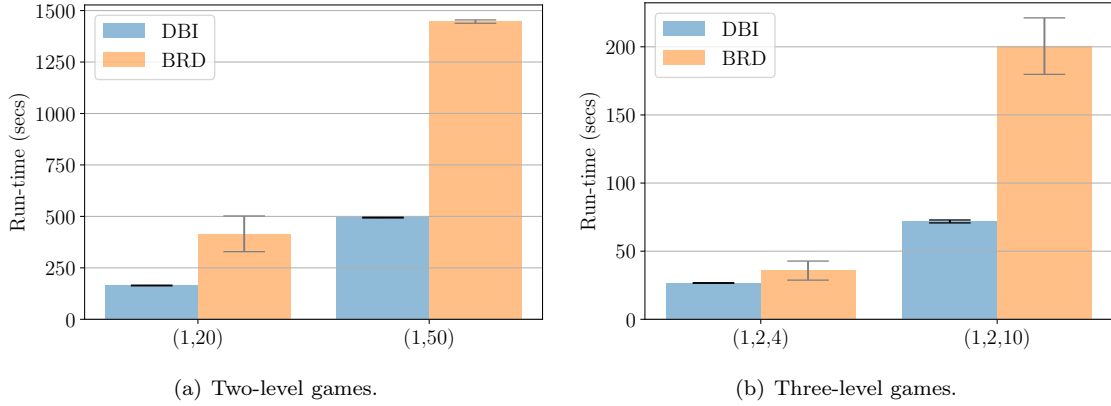


Figure 6: The run-time (in secs) on COVID-19 Game Models. $T = 20$ for BRD experiments.

projected gradient descent method, if all the gradients go to zero, DBI converges. Besides, it is also likely to hit the boundary of the constraints. The DBI is possible to converge with a non-zero gradient norm. The BRD algorithm terminates either T achieves, or ϵ goes to zero for all players. Under these conditions, the two algorithms find their optimal solutions. Figure 6 demonstrates the run-time results. We conduct each experiment four times with different random seeds. In two-level problems, the DBI algorithm is more than two times faster than BRD algorithms. Although the action spaces are discretized to 11 grid points for three-level games rather than 101 grids, DBI algorithms still perform better. In practice, discretizing the action spaces in 101 grids for three-level games is computationally intensive. The performance and run-time of the BRD algorithm are more dependent on randomization and the initial points for the best responses at each level. When we face many players or multiple levels, the DBI algorithm is a natural choice. The DBI algorithm is significantly more efficient and more stable than the BRD algorithm.

B.5 Additional Experiments on the Relationship Between LASP and LSPE

In this additional experiment, We will study the chance of having a convergent algorithm as well as the probability of finding an equilibrium upon convergence on several classes of SHGs. We design game classes of SHGs in a way that every game class \mathcal{F} has the same parameter space on both its topology and payoff structure. For each class, we generate N instances, and for each instance, we first find the set of critical

points by numerically solving the first order condition $D_{\mathbf{x}_{l,i}} u_{l,i} = 0, \forall(l, i)$. For each of these critical points, we determine whether it is an LASP of DBI by checking whether the Jacobian of updating gradient G have eigenvalues all of which have negative real part. If this is the case, we classify the critical point as an LASP according to Proposition 1. Finally, for each of the LASPs, we further check whether it is an LSPE by checking whether $D_{\mathbf{x}_{l,i}, \mathbf{x}_{l,i}}^2 u_{l,i} < 0, \forall(l, i)$. Finally, across the N instances we compute the fraction of games for which an LASP was found (% LASP), and for those with an LASP, the fractions of the instances where an LASP is also an LSPE (% LSPE). We call these two numbers the measure properties of a game class.

We denote by our game classes by $\mathcal{F}_{\text{sub}}^{\text{super}}$ where the subscript is a vector listing the number of players in each SHG layer from top to bottom, and the superscript indicates the parameters of the game. For example $\mathcal{F}_{1,1}^C$ is an SHG class with two layers and one player in each level (a Stackelberg game) with $C \in \mathbb{R}^+$ determining payoffs as follows: $u_i = \sum_{\alpha+\beta \leq 4, \alpha, \beta \in \mathbb{N}} c_{i,\alpha,\beta} x^\alpha y^\beta$, where $x, y \in \mathbb{R}$ are 1-d action variables for the player ($i = 1$) and the second layer-2 player ($i = 2$), respectively; the player-specific coefficients $c_{i,\alpha,\beta}$ are integers generated uniformly in $[-C, C]$ for different values of C . When $C = \infty$, we generate the coefficients from a continuous uniform distribution in $[-1, 1]$. See Appendix B for more information (e.g., the utility structure) of the other game classes.

| \mathcal{F} | $\mathcal{F}_{1,1}^1$ | $\mathcal{F}_{1,1}^{10}$ | $\mathcal{F}_{1,1}^\infty$ | $\mathcal{F}_{1,2}^1$ | $\mathcal{F}_{1,2}^{10}$ | $\mathcal{F}_{1,2}^\infty$ | $\mathcal{F}_{1,1,1}^1$ | $\mathcal{F}_{1,1,1}^{10}$ | $\mathcal{F}_{1,1,1}^\infty$ | $\mathcal{F}_{1,1,2}^1$ | $\mathcal{F}_{1,1,2}^{10}$ | $\mathcal{F}_{1,1,2}^\infty$ |
|---------------|-----------------------|--------------------------|----------------------------|-----------------------|--------------------------|----------------------------|-------------------------|----------------------------|------------------------------|-------------------------|----------------------------|------------------------------|
| % LASP | 52.6 | 57.3 | 59.7 | 32.0 | 35.0 | 36.8 | 47.0 | 51.0 | 50.3 | 13.6 | 21.3 | 21.2 |
| % LSPE | 88.8 | 87.9 | 87.1 | 65.6 | 64.3 | 60.0 | 66.5 | 64.3 | 67.0 | 62.1 | 60.7 | 60.2 |

Table 2: Results for $\mathcal{F}_{1,1}^C$, $\mathcal{F}_{1,2}^C$, $\mathcal{F}_{1,1,1}^C$ and $\mathcal{F}_{1,1,2}^C$ averaged over $N = 10^5$ instances.

The results are shown in Table 2. First, we notice for the same game topology, C does not appear to substantially affect the measure property. Parameter C essentially controls the granularity of a uniform discrete distribution and approaches a uniform continuous distribution as it becomes large. The measure properties will also be quite similar as C grows. The second observation is that as the topology becomes much more complex, it is less probable for DBI to find a stable point. The relevant probabilities degrade from 52% \sim 59% for Stackelberg games to 13% \sim 21% for 4-player 3-level games. This suggests a limitation of our algorithm in facing complex game topologies with more intricate back-propagation. However, we observe that the probability of an LASP being an LSPE does not decay speedily, as it achieves 87% \sim 88% for the structure of (1, 1), 60% \sim 67% for (1, 2), (1, 1, 2) and (1, 1, 1).

B.6 Details of The Experiment

We elaborate our experimental designs here. For each function class \mathcal{F} , we generates N instances. For each instances, we solve equations $D_{\mathbf{x}_{l,i}} = 0, \forall(l, i)$, using numerical methods provided by Mathematica [52]. For each critical point found, we check whether the Jacobian of the updating gradient has eigenvalues all of which have negative real parts. If it is the case, we classify it as an LASP. For each of such LASP, we can determine whether it is an LSPE by checking whether $D_{\mathbf{x}_{l,i}, \mathbf{x}_{l,i}}^2 < 0$. Then for each instance, we can have two numbers: (1) an indicator demonstrating whether it is found an LASP (2) if there is an LASP, the fraction of these LASPs being LSPE. Then across these N instances, we define $\%LASP \triangleq \#(\text{Instances found LASP})/N$ and $\%LSPE \triangleq \sum(\text{Fraction of these LASPs being LSPE in an instance})/\#(\text{Instances found LASP})$.

$\mathcal{F}_{1,1}^C$ is detailed in the main body. For $\mathcal{F}_{1,2}^C$, the payoff structure is $u_{1,1}(x, y, z) = \sum_{\alpha+\beta+\gamma \leq 3, \alpha, \beta, \gamma \in \mathbb{N}} c_{(1,1), \alpha, \beta, \gamma} x^\alpha y^\beta z^\gamma$, $u_{2,1}(x, y, z) = \sum_{\alpha+\beta+\gamma \leq 3, \alpha, \beta, \gamma \in \mathbb{N}} c_{(2,1), \alpha, \beta, \gamma} x^\alpha y^\beta z^\gamma$, $u_{2,2}(x, y, z) = \sum_{\alpha+\beta+\gamma \leq 3, \alpha, \beta, \gamma \in \mathbb{N}} c_{(2,2), \alpha, \beta, \gamma} x^\alpha y^\beta z^\gamma$, where x, y, z are action variables for players (1, 1), (2, 1), (2, 2) respectively.

For $\mathcal{F}_{1,1,1}^C$, $u_1(x, z) = \sum_{\alpha+\beta \leq 4, \alpha, \beta \in \mathbb{N}} c_{1, \alpha, \beta} x^\alpha z^\beta$, $u_2(x, y, z) = \sum_{\alpha+\beta+\gamma \leq 3, \alpha, \beta, \gamma \in \mathbb{N}} c_{2, \alpha, \beta, \gamma} x^\alpha y^\beta z^\gamma$, $u_3(y, z) = \sum_{\alpha+\beta \leq 4, \alpha, \beta, \gamma \in \mathbb{N}} c_{3, \alpha, \beta, \gamma} y^\alpha z^\beta$, where x, y, z are action variables for players (1, 1), (2, 1), (3, 1) respectively.

For $\mathcal{F}_{1,1,2}^C$, $u_{1,1}(x, y, z) = \sum_{\alpha+\beta+\gamma \leq 3, \alpha, \beta, \gamma \in \mathbb{N}} c_{1, \alpha, \beta, \gamma} x^\alpha y^\beta z^\gamma$, $u_{2,1}(w, x, y, z) = \sum_{\alpha+\beta+\gamma+\iota \leq 2, \alpha, \beta, \gamma, \iota \in \mathbb{N}} c_{2, \alpha, \beta, \gamma, \iota} x^\alpha y^\beta z^\gamma w^\iota$, $u_{3,1}(w, y, z) = \sum_{\alpha+\beta+\gamma \leq 3, \alpha, \beta, \gamma \in \mathbb{N}} c_{(3,1), \alpha, \beta, \gamma} w^\alpha y^\beta z^\gamma$, $u_{3,2}(w, y, z) = \sum_{\alpha+\beta+\gamma \leq 3, \alpha, \beta, \gamma \in \mathbb{N}} c_{(3,2), \alpha, \beta, \gamma} w^\alpha y^\beta z^\gamma$, where (x, w, y, z) are action variables for players (1, 1), (2, 1), (3, 1), (3, 2).